DOKUZ EYLÜL UNIVERSITY

GRADUATE SCHOOL OF NATURAL AND APPLIED SCIENCES

DETERMINATION OF THE SURFACE ACIDITIES OF VARIOUS CATALYSTS

by

Hasibe SANDIKÇIOĞLU

June, 2011

İZMİR

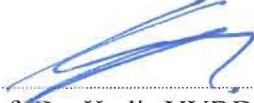# DETERMINATION OF THE SURFACE ACIDITIES OF VARIOUS CATALYSTS

A Thesis Submitted to the
Graduate School of Natural and Applied Sciences of
Dokuz Eylül University
In Partial Fulfillment of the Requirements for
The Degree of Master of Science in Chemistry Program

by
Hasibe SANDIKÇIOĞLU

June, 2011
İZMİR

M. Sc. THESIS EXAMINATION RESULT FORM

We have read the thesis entitled **"DETERMINATION OF THE SURFACE ACIDITIES OF VARIOUS CATALYSTS"** completed by **HASİBE SANDIKÇIOĞLU** under supervision of **PROF. DR. KADİR YURDAKOÇ** and we certify that in our opinion it is fully adequate, in scope and in quality, as a thesis for the degree of Master of Science.

Prof. Dr. Kadir YURDAKOÇ

Supervisor

Prof. Dr. Melek MERDIVAN

(Jury Member)

Assist. Prof. Dr. Ehver Yaser KÜÇÜKGÜL

(Jury Member)

Prof. Dr. Mustafa SABUNCU

Director Graduate School of Natural and Applied Sciences

ACKNOWLEDGMENTS

I would like to express my gratitude to my supervisor, Prof. Dr. Kadir YURDAKOÇ for his guidance, encouragement and support. It was a privilege to study under his supervision.

Also, I would like to thank to Res. Assist. Aylin ALTINIŞIK for her precious suggestions and discussions during the preparation of the thesis.

In addition, I wish to express my gratefulness to all friends for their continuous helpful encouragement and valuable supports.

Finally, I would like to thank my family for bringing me in this situation with their unique patience and supports.

<div align="right">

Hasibe SANDIKÇIOĞLU

</div>

DETERMINATION OF THE SURFACE ACIDITIES OF VARIOUS CATALYSTS

ABSTRACT

The surface acidities of various Silica-Alumina, Sepiolite and Bentonite catalysts were determined by way of n-butyl amine titration technique with Hammett indicators in nonaqueous solvents such as benzene, back titration with sodium bicarbonate, sodium carbonate and sodium hydroxide bases in aqueous solution. Surface functional groups of various Silica-Alumina, Sepiolite and Bentonite catalysts were also investigated by Boehm's titration technique. The points of zero charges were determined as neutral and acidic pH. Furthermore, the Brønsted and Lewis acid sites of the catalysts were investigated after the adsorption of pyridine in gas phase by FTIR spectroscopic method of analysis. The calculated total amount of acid of Silica-Alumina samples increased with the increase in silicon dioxide content up to Siral 40 and then decreased sharply in the case of Siral 80. FTIR spectroscopy was used successfully with pyridine as a basic probe, to determine the Brønsted and Lewis acid sites on the surface of various Silica-Alumina, Sepiolite and Bentonite catalysts. All samples have both Lewis and Brønsted acidity. The Lewis sites predominate in all the silica-aluminas.

Keywords: surface acidity, Hammett acidity function, n-butyl amine titration, pyridine adsorption, FTIR spectroscopy

ÇEŞİTLİ KATALİZÖRLERİN YÜZEY ASİTLİKLERİNİN BELİRLENMESİ

ÖZ

Çeşitli Siral (silika-alumina) bileşikleri, Bentonit ve Sepiyolit katalizörlerinin yüzey asitlikleri, Hammett indikatörleri yardımıyla susuz ortamda (Benzen) n-bütil amin titrasyonuyla, sulu ortamda da çeşitli indikatörlerle sodyum bikarbonat, sodyum karbonat, sodyum hidroksit gibi bazlarla geri titrasyon yöntemiyle belirlenmiştir. Çeşitli Siral (silika-alumina) bileşikleri, Bentonit ve Sepiyolit katalizörlerinin yüzey fonksiyonel grupları Boehm titrasyon tekniği ile araştırılmıştır. Yüzey net yükleri, asidik ve nötral pH olarak belirlenmiştir. Ayrıca gaz fazında piridin adsorpsiyonları yapılarak FTIR spektroskopisi yöntemiyle katalizörlerin Lewis ve Brønsted asit merkezleri belirlenmeye çalışılmıştır. Siral örneklerinde, asitliğin artan silisyum dioksit içeriği miktarıyla Siral 40'a kadar arttığı, Siral 80 de ise azaldığı görülmektedir. Yüzey üzerindeki Lewis ve Brønsted asit merkezlerini belirlemek için kullanılan FTIR spektroskopisiyle gaz fazında piridin adsorpsiyonunda bütün örneklerin Lewis ve Brønsted asit merkezlerine sahip oldukları görülmektedir. Tüm silika-alumina bileşiklerinde Lewis asit merkezlerinin baskın olduğu görülmüştür.

Anahtar sözcükler: yüzey asitliği, Hammett asitlik fonksiyonu, n-butil amin titrasyonu, piridin adsorpsiyonu, FTIR spektroskopisi

CONTENTS   **Page**

CHAPTER ONE

INTRODUCTION

1.1 Solid Acids and Bases

There are many definitions of acids and bases in the literature, notably those of Franklin (Franklin, 1905), Brønsted (Brønsted, 1926), Germann (Germann, 1925), Lewis (Lewis, 1938), Bjerrum (Bjerrum & Sansoni,1951), Johnson (Johnson, Norris & Huston, 1951), Lux, Flood et al., and Tomlinson (Flood & Förland, 1947), and Pearson (Pearson, 1963). We may understand a solid acid in general terms as a solid on which the colour of a basic indicator changes, or as a solid on which a base is chemically adsorbed. More strictly, following both the Brønsted and Lewis definitions, a solid acid shows a tendency to donate a proton or to accept an electron pair, where as a solid base tends to accept a proton or to donate an electron pair. These definitions are adequate for an understanding of the acid base phenomena shown by various solids, and are convenient for the clear description of solid acid and base catalysis (Tanebe, Misono, Ono, & Hattori, 1989).

In accordance with the above definitions a summarized list of solid acids and bases is given here in Tables 1.1 and 1.2.

The first group of solid acids, which includes naturally occurring clay minerals, has the longest history. Some were investigated as long ago as the turn of the century, and especially since the 1920's there have been numerous studies of their catalytic activities, although only recently have investigations commenced on zeolites. The main constituents of the first group of solid acids are silica and alumina. The very well-known solid acid catalyst synthetic silica-alumina is listed in the 4th group, which also includes the many oxide mixtures which have recently been found to display acidic properties and catalytic activity. In the 5th group are included many

1

inorganic chemicals such as the metal oxides, sulfides, sulfates, nitrates and phosphates. Many in this group have recently been found to show characteristic selectivities as catalysts.

Table 1.1 Solid acids (Tanabe, Misono, Ono, & Hattori, 1989)

1. Natural clay minerals: kaolinite, bentonite, attapulgite, montmorillonite, clarit, Fuller's earth, zeolites (X, Y, A. H-ZSM etc), cation exchanged zeolites and clays
2. Mounted acids: H_2SO_4, H_3PO_4, H_3BO_3, $CH_2(COOH)_2$ mounted on silica, quartz sand, alumina or diatomaceous earth
3. Cation exchange resins
4. Charcoal (heat-treated at 573 K)
5. Metal oxides and sulphides: ZnO, CdO, Al_2O_3, CeO_2, ThO_2, TiO_2, ZrO_2, SnO_2, PbO, As_2O_3, Bi_2O_3, Sb_2O_5, V_2O_5,Cr_2O_3, MoO_3, CdS, ZnS
6. Metal Salts: $MgSO_4$, $CaSO_4$, $SrSO_4$, $BaSO_4$, $CuSO_4$, $ZnSO_4$, $CdSO_4$, $Al_2(SO_4)_3$, $Fe_2(SO_4)_3$, $CoSO_4$, $NiSO_4$, $Cr_2(SO_4)_3$, $KHSO_4$, K_2SO_4, $(NH_4)_2SO_4$, $Zn(NO_3)_2$, $Ca(NO_3)_2$, $Bi(NO_3)_3$, $Fe(NO_3)_3$, $CaCO_3$, BPO_4, $AlPO_4$, $CrPO_4$, $FePO_4$, $Cu_3(PO_4)_2$, $Zn_3(PO_4)_2$, $Mg_3(PO_4)_2$, $Ti_3(PO_4)_4$, $Zr_3(PO_4)_2$, $Ni_3(PO_4)_2$, AgCl, CuCl, $SnCl_2$, $CaCl_2$, $AlCl_3$, $TiCl_3$, CaF_2, BaF_2, $AgClO_4$, $Mg_2(ClO_4)_2$
7. Mixtures of oxides: Mixed oxides : SiO_2-Al_2O_3, SiO_2-TiO_2, SiO_2-SnO_2, SiO_2-ZrO_2, SiO_2-BeO, SiO_2-MgO, SiO_2-CaO, SiO_2-SrO, SiO_2-ZnO, SiO_2-Ga_2O_3, SiO_2-Y_2O_3, SiO_2-La_2O_3, SiO_2-MoO_3, SiO_2-WO_3, SiO_2-V_2O_5, SiO_2-ThO_2, Al_2O_3-MgO, Al_2O_3-ZnO, Al_2O_3-CdO, Al_2O_3-B_2O_3, Al_2O_3-ThO_2, Al_2O_3-TiO_2, Al_2O_3-ZrO_2, Al_2O_3-V_2O_5, Al_2O_3- MoO_3, Al_2O_3-WO_3, Al_2O_3-Cr_2O_3, Al_2O_3-Mn_2O_3, Al_2O_3-F_2O_3, Al_2O_3-Co_3O_4, AI_2O_3-NiO, TiO_2-CuO, TiO_2-MgO, TiO_2-ZnO, TiO_2-CdO, TiO_2-ZrO_2, TiO_2-SnO_2, TiO_2-Bi_2O_3, TiO_2-Sb_2O_5, TiO_2-V_2O_5, TiO_2-Cr_2O_3, TiO_2-MoO_3, TiO_2-WO_3, TiO_2-Mn_2O_5, TiO_2-Fe_2O_3, TiO_2-Co_3O_4, TiO_2-NiO, ZrO_2-CdO, ZnO-MgO, ZnO-Fe_2O_3, MoO_3-CoO-Al_2O_3, MoO_3-NiO-Al_2O_3, TiO_2-SiO_2-MgO, MoO_3-Al_2O_3-MgO, heteropoly acids

Of the solid bases listed in Table 1.2 special mention should perhaps be made of the alkaline earth metal oxides in the 4th group, whose basic properties and catalytic action have recently been investigated. The fact that alumina, zinc oxide and silica-

alumina show both acidic basic properties is of special significance for acid-base bifunctional catalysis.

Table 1.2 Solid bases (Tanabe, Misono, Ono, & Hattori, 1989)

1. Mounted bases: NaOH, KOH mounted on silica or alumina; Alkali metal and alkaline earth metal dispersed on silica, alumina, carbon, K_2CO_3 or in oil; NR_3, NH_3, KNH_2 on alumina; Li_2CO_3 on silica; t-BuOK on xonotolite
2. Anion exchange resins
3. Charcoal (heat-treated at 1173 K or activated with N_2O, NH_3 or $ZnCl_2$-NH_4Cl-CO_2)
4. Metal oxides: BeO, MgO, CaO, SrO, BaO, ZnO, Al_2O_3, Y_2O_3, La_2O_3, CeO_2, ThO_2, TiO_2, ZrO_2, SnO_2, Na_2O, K_2O
5. Metal salts: Na_2CO_3, K_2CO_3, $KHCO_3$, $KNaCO_3$, $CaCO_3$, $SrCO_3$, $BaCO_3$, $(NH_4)_2CO_3$, $Na_2WO_4 \cdot 2H_2O$, KCN
6. Mixed oxides: SiO_2-MgO, SiO_2-CaO, SiO_2-SrO, SiO_2-BaO, SiO_2-ZnO, SiO_2-Al_2O_3, SiO_2-ThO_2, SiO_2-TiO_2, SiO_2-ZrO_2, SiO_2-MoO_3, SiO_2-WO_3, Al_2O_3-MgO, Al_2O_3-ThO_2, Al_2O_3-TiO_2, Al_2O_3-ZrO_2, Al_2O_3-MoO_3, Al_2O_3-WO_3, ZrO_2-ZnO, ZrO_2-TiO_2, TiO_2-MgO, ZrO_2-SnO_2
7. Various kinds of zeolites exchanged with alkali metal or alkaline earth metal

A solid superacid is defined as a solid whose acid strength is higher than the acid strength of 100% sulfuric acid. Since the acid strength of 100% sulfuric acid expressed by the Hammett acidity function, H_0, is -11.9, a solid of $H_0 < -11.9$ is called a solid superacid. The kinds of solid superacids are shown in Table 1.3. The groups 1 through 6 include acids supported on various solids.

On the other hand, a solid superbase is defined as a solid whose base strength expressed by the basicity function, H-, is higher than + 26. The basis of the definition has been described in literature (Tanabe, 1985). The kinds of solid superbases are shown in Table 1.4 together with their preparation method and pretreatment temperature.

Table 1.3 Solid Superacids (Tanabe, Misono, Ono, & Hattori, 1989)

Group	Acid	Support
1a	SbF_5	SiO_2-Al_2O_3, SiO_2-TiO_2, SiO_2-ZrO_2, TiO_2-ZrO_2
1b	SbF_5	Al_2O_3-B_2O_3, SiO_2, SiO_2- WO_3, HF-Al_2O_3
2	SbF_5, TaF_5	Al_2O_3, MoO_3, ThO_2, Cr_2O_3, AI_2O_3-WB
3	SbF_5, BF_3	graphite, Pt-graphite
4	BF_3, $AlCl_3$, $AlBr_3$	ion exchange resin, sulfate, chloride
5	SbF_5-HF SbF_5-FSO_3-H	metal (Pt, Al), alloy (Pt-Au, Ni-Mo, Al-Mg), polyethylene, SbF_3, AlF_3, porous substance(SiO_2-Al_2O_3, kaolin, active carbon, graphite)
6	SbF_5-CF_3SO_3H	F-Al_2O_3, $AlPO_4$, charcoal
7	Nafion (polymeric perfluororesin sulfonic acid)	
8	TiO_2-SO_4^{-2}, ZrO_2- SO_4^{-2}, Fe_2O_3- SO_4^{-2}	
9	H-ZSM-5 zeolite	

Table 1.4 Solid Superbases (Tanabe, Misono, Ono, & Hattori, 1989)

	Starting material, Preparation method	Pretreatment temp. K	H_
CaO	$CaCO_3$	1173	26.5
SrO	$Sr(OH)_2$	1123	26.5
MgO-NaOH	(NaOH impregnated)	823	26.5
MgO-Na	(Na vaporized)	923	35
Al_2O_3-Na	(Na vaporized)	823	35
Al_2O_3-NaOH-Na	(NaOH, Na impregnated)	773	37

1.2 Determination of Acidic Properties on Solid Surfaces

A complete description of acidic properties on solid surfaces requires the determination of the acid strength, and of the amount and nature (Brønsted or Lewis acid type) of the acid centers.

1.2.1 The Acid Strength and Amount of Solid Acids

The acid strength of a solid is the ability of the surface to convert an adsorbed neutral base into its conjugate acid as described by Walling (1950). If the reaction proceeds by means of proton transfer from surface to the adsorbate, the acid strength is expressed by the Hammett acidity function H_0 (Hammett & Deyrup, 1932),

$$H_0 \equiv -\log a_{H^+} f_B / f_{BH^+} \qquad \text{(Eq. 1.1)}$$

or

$$H_0 \equiv pKa + \log [B] / [BH^+] \qquad \text{(Eq. 1.2)}$$

Where is a_{H^+} the proton activity, and [B] are [BH$^+$] respectively the concentrations of the neutral base and its conjugate acid, and f_B and f_{BH^+} the corresponding activity coefficients. If the reaction takes place by means of electron pair transfer from the adsorbate to the surface, H_0 is expressed by

$$H_0 \equiv -\log a_A f_B / f_{AB} \qquad \text{(Eq. 1.3)}$$

or

$$H_0 \equiv pKa + \log [B] / [AB] \qquad \text{(Eq. 1.4)}$$

Where a_A is the activity of the Lewis acid or electron pair acceptor, A. [AB] is the concentration of the Lewis acid interacting with neutral base.

The amount of acid on a solid is usually expressed as the number or mmol of acid sites per unit weight or per unit surface area of the solid, and is obtained by measuring the amount of a base which reacts with the solid acid. It is also sometimes

loosely called "acidity". There are basically two methods for the determination of acid strength and amount of a solid acid. These are an amine titration method (n-butyl amine titration) using Hammett indicators and a gaseous base adsorption method (pyridine adsorption) (Tanebe, Misono, Ono, & Hattori, 1989).

1.2.1.1 Amine Titration Method with Using Indicators

The colour of suitable indicators adsorbed on a surface will give a measure of its acid strength. If the colour is that of the acid form of the indicator, then the values of the H_0 function of the surface is equal to or lower than the pKa of the indicator. Lower values of H_0, of course, correspond to greater acid strength. Thus for indicators undergoing colour changes in this way, the lower the pK_a, the greater is the acid strength of the solid. For example, a solid which gives a yellow colouration with benzalacetophenone ($pK_a = -5.6$), but is colourless with anthraquinone ($pK_a = -8.2$), has an acid strength of H_0 which lies between -5.6 and -8.2. A solid having $H_0 \leq -16.04$ will change all indicators given in 2.1 from the basic to the acidic colours, whereas one which changed none of them would have an acid strength as $H_0 = +6.8$ or even less ($H_0 > +6.8$).

The determination is made by placing about 0.2 mg of the sample in powder form into a test tube, adding 2 mL of non-polar solvent containing about 0.2 mg of indicator, and shaking briefly. If the adsorption occurs at all and proceeds very rapidly, then the change in colour between basic and acidic forms of the indicator is most striking. Experimental details are given in the literature (Tanabe, 1970; Tanabe, Anderson, & Boudart, 1981).

The acid strength of a solid superacid which is very sensitive to moisture can be determined by observing the color change of an indicator whose vapor is absorbed on a solid sample through a breakable seal in a vacuum system at room temperature (Tanabe & Hattori, 1976).

The amount of acid sites on a solid surface can be measured by amine titration immediately after determination of acid strength by the above method. The method consists of titrating a solid acid suspended in benzene with n-butyl amine, using an indicator.

Table1.5 Basic indicators used for the measurement of acid strength (Tanabe, Misono, Ono, & Hattori, 1989)

Indicators	Color		pK_a[1]	$[H_2SO_4]$[2]/%
	Base-form	Acid-form	pK_a	
Neutral red	yellow	red	+6.8	8.10^{-8}
Methyl red	yellow	red	+4.8	-
Phenylazonaphtylamine	yellow	red	+4.0	5.10^{-5}
p-Dimethylaminoazobenzene	yellow	red	+3.3	3.10^{-4}
2-Amino-5-azotoluene	yellow	red	+2.0	5.10^{-3}
Benzeneazodiphylamine	yellow	purple	+1.5	2.10^{-2}
Crystal violet	blue	yellow	+0.8	0.1
p-Nitrobenzeneazo-(p'-nitro-dipehylamine)	orange	purple	+0.43	-
Dicinnamalacetone	yellow	red	-3.0	48
Benzalacetophenone	colorless	yellow	-5.6	71
Anthraquinone	colorless	yellow	-8.2	90
2,4,6-Trinitroaniline	colorless	yellow	-10.10	98
p-Nitrotoluene	colorless	yellow	-11.35	*
m-Nitrotoluene	colorless	yellow	-11.99	*
p-Nitrofluorobenzene	colorless	yellow	-12.44	*
p-Nitrochlorobenzene	colorless	yellow	-12.70	*
m-Nitrochlorobenzene	colorless	yellow	-13.16	*
2,4-Dinitrotoluene	colorless	yellow	-13.75	*
2,4-Dinitrofluorobenzene	colorless	yellow	-14.52	*
1,3,5-Trinitrotoluene	colorless	yellow	-16.04	*

[1] pK_a, of the conjugate acid, BH^+, of indicator, B, $(= pK_{BH}^+)$
[2] wt, percent of H_2SO_4 in sulfuric acid solution which has the acid strength corresponding to the respective pK_a
[3] The indicator is liquid at room temperature and acid strength corresponding to the indicator is higher than the acid strength of 100 percent H_2SO_4 .

The amine titration method gives the sum of the amounts of both Brønsted and Lewis acid, since both proton donors and electron pair acceptors on the surface will react with either the electron pair $(-\overset{..}{N}=)$ of the indicator or that of amine $(= N:)$ to form a coordination bond. This method is rarely applied to colored or dark samples where the usual color change is difficult to observe. However, the difficulty can be minimized by mixing a white substance of known acidity with the sample or by employing the spectrophotometric method (Tanabe et al., 1981).

1.2.1.2 Adsorption of Pyridine in Gas Phase Method

The adsorption of bases is widely used for the determination of the acidity of solid surfaces. Amines, as ammonia, pyridine or aliphatic amines are the bases most often used in adsorption measurements. The center of basicity is the electron lone pair on the nitrogen, which also makes amines active ligands in various complexes. When chemisorbed on a surface, possessing acid properties, amines can interact with acidic protons, electron acceptor sites, and hydrogen from neutral or weakly acidic hydroxyls (Kijenski & Baiker, 1989).

Pyridine is considered to be a much more selective indicator for surface acidity (Parry, 1963). Pyridine is a strong base (pK_B = 8.75) and exhibits a high affinity for the formation of complexes and is also an active acceptor for the hydrogen bond (Lindemann & Zundel, 1977); hence also the latter type of interaction can affect its chemisorption properties.

Pyridine adsorption onto solid surfaces monitored by IR spectroscopy has been a generally accepted and applied method for determining the acidity of solids for a long time (Richardson & Benson, 1957; Basila et al., 1964; Bourne, Cannings, & Pitkethly, 1970; Cannings, 1968). Parry (1963) first showed that the IR spectrum of pyridine adsorbed on metal oxides allows one to clearly distinguish the nature of acidic sites (Lewis-Brønsted) from the study of the $v(C==C)$ ring vibrations in the 1400- 1700 cm^{-1} range. The types of site affecting adsorption were classified as Lewis (LPY), Brønsted (BPY) and surface hydroxyl (HPY). Parry (1963) utilized the

fact that pyridine interacting as a Lewis base (LPY) has a distinctly different spectrum from that of pyridine interacting as a Brønsted base (BPY) (Gill, Nuttall, Scaife, & Sharp, 1961; Cook, 1961). Parry's results indicate that only Lewis sites are present on alumina while both Lewis and Brønsted sites observed on silica-alumina (Parry, 1963). Generally two bands are observed, which are attributed to pyridine-acid sites interaction (Parry, 1963): the absorption of pyridinium ions (generated by interaction of pyridine with Brønsted acid sites) at 1540 cm^{-1}, and that of the coordinatively bonded pyridine complexes (formed in the interaction between pyridine and Lewis acid sites) at 1455 cm^{-1}.

The presence of physically adsorbed pyridine (PY) which is apparently held on the surface by a hydrogen-bonding interaction with surface OH groups is detected by the observation of the characteristic 1593 and 1614 cm^{-1} (Basila, Kantner, & Rhee, 1964). Chemisorbed pyridine interacting as a Brønsted base (BPY) is characterized by the bands at 3260 and 3188 cm^{-1} which are due to NH^{+} stretching vibration(Cook, 1961) and by the bands at 1638 and 1545 cm^{-1} which are due to the combined C-C stretching and in-plane CH and NH bending modes (Cook, 1961; Zerbi, Crawford, & Overend, 1963). Table 1.6 lists the assignments of the different bands; the 19b modes were used to distinguish between different types of adsorbed pyridine (Bourne, Cannings, & Pitkethly, 1970; Basila & Kantner, 1966).

Table 1.6 Pyridine Assignments for the evaluation of the data in the range 1700-1400 cm^{-1}

Type	PY cm^{-1}	HPY cm^{-1}	BPY cm^{-1}	LPY cm^{-1}
Mode 8a	1582	1614	1639	1617
8b	-	1593	1613	-
19a	1483	1490	1489	1495
19b	1440	1438	1539	1451

It is to be noted; irreversibly adsorbed H$_2$O converts Lewis sites to Brønsted sites (Basila, Kantner, & Rhee, 1964; Bourne, Cannings, & Pitkethly, 1970; Parry, 1963). A progressive dehydration of acidic solids may occur during heating, with consequent transformation of Brønsted into Lewis acid sites, according to reaction (Barzetti, Selli, Moscotti, & Forni, 1996),

Brønsted site   Lewis site
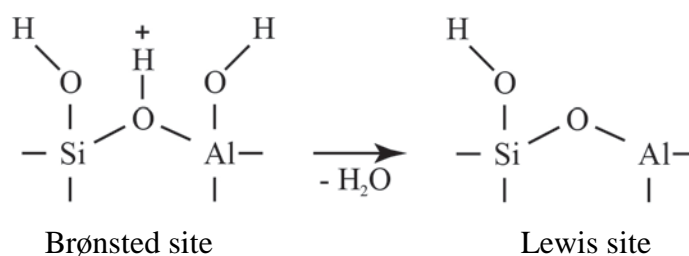
The ratio of the absorption coefficients of characteristic bands of chemisorbed LPY and BPY should be known, in order to determine the quantitative amount of Lewis and Brønsted acid sites. The band at 1450 cm^{-1} (for 19b mode of PYL) and the band at 1545 cm^{-1} (for BPY species) were taken to be identical with the ratio of absorption coefficients of characteristic bands of chemisorbed LPY and BPY. The most reliable value was calculated on Hughes and White's (1967) data.

$$\varepsilon_{1450} / \varepsilon_{1545} = 1.08 \pm 0.09 \qquad \text{(Eq. 1.5)}$$

However, Basila et al. (1966) calculated the above ratio as 1.6±0.3.

It is proposed that all of the primary acid sites on a silica- alumina are of the Lewis type centered on active surface Al atoms. Brønsted acidity occurs by a "second – order" interaction between the molecules chemisorbed on the Lewis type site and a nearby surface OH group. This interaction between the surface OH group and the chemisorbed molecule is essentially a hydrogen-bonding interaction (Basila, Kantner, & Rhee, 1964).

1.2.1.3 Determination of the Acidity in Aqueous Solution with Bases by the back-titration Method

Surface functional groups on samples were determined by Boehm's titration (Boehm, 1994; Toles, Marshall, & Johns, 1999). In this method, certain titrable surface functional groups on the samples can be determined and quantify the amount of various types of oxygenated groups.

Initially, acid sites on surface are neutralized by excess $NaHCO_3$, Na_2CO_3, NaOH base solutions in aqueous solution. Then the remaining bases are back- titrated with a standardized HCl solution. The numbers of acidic sites of various types were calculated using the assumptions that NaOH neutralizes carboxylic, phenolic, and lactonic groups, Na_2CO_3 neutralizes carboxylic and lactonic groups, and $NaHCO_3$ neutralizes only carboxylic groups (Boehm, 1994).

1.3 Silica-Alumina Catalysts

The chemistry of both silica and alumina in the solid state has been applied to the silica-alumina cracking catalyst. This resulted in the hypothesis that the active part of the catalyst is formed when one aluminum atom shares four oxygen atoms which in turn are shared by four silicon atoms. An acidic hydrogen ion is thought to be associated with the four oxygen atoms surrounding the aluminum atom. The catalytic activity is ascribed to this acidic hydrogen. The formula for the active part of the catalyst has been written $(HAlSiO_4)_x$ where x indicates that it is a part of a solid which may have the same or a different composition. The nature of $(HAlSiO_4)_x$ is such that it cannot exist as the monomer, $HAlSiO_4$. The logic built up in the hypothesis leads to the conclusion that, for maximum activity, the catalyst should have a composition in which the atomic ratio of silica to alumina is one. To obtain maximum activity these catalysts should be made in special ways. Silica-alumina catalysts of maximum activity probably cannot be prepared by forming a silica hydrogel and depositing alumina on it.

The following known facts regarding synthetic silica-alumina catalysts have been examined in the light of the chemistry of solids. The results of the examination, reported here, lead to the hypothesis that the catalytic activity is due to hydrogen ions present in the catalysts. It is hoped that the material presented will prove to be a step toward answering the question of what makes a cracking catalyst crack. Silica alone is either inactive or only slightly active as a cracking catalyst. Alumina alone is better than silica but is an inferior cracking catalyst. The proper combination of silica-alumina is very much more active than either of its components. Silica-alumina

catalysts are prepared from the hydrogels or hydrous oxides. The mixtures of the anhydrous oxide with one hydrous oxide do not produce an active catalyst. The silica-alumina catalyst apparently has certain acidic properties. The catalysts are solids.
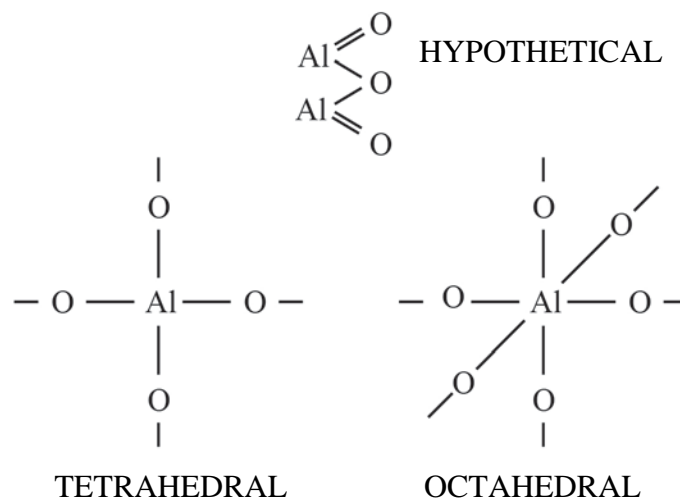
Solids have structures in much the same sense that organic molecules have structure. It is important to realize that there is no such thing as O=Si=O in the solid state. Rather, each silicon atom is attached to four oxygen atoms and these oxygen atoms are equidistant from the silicon. The centers of the oxygen atoms are located at the corners of a tetrahedron with the silicon in the center:

$$SiO_2$$

O=Si=O (HYPOTHETICAL)

$$
\begin{array}{c}
\mid \\
O \\
\mid \\
- O - Si - O - \\
\mid \\
O \\
\mid
\end{array}
$$
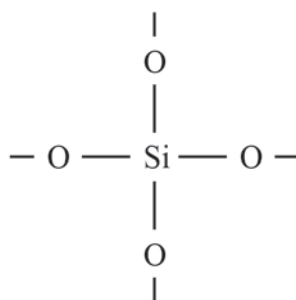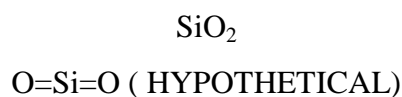
TETRAHEDRAL

This arrangement for silicon and oxygen is characteristic of all known crystalline forms of silica and for all solid inorganic silicates. This unit is then a monomer or building unit from which solids are built.

Aluminum, in some compounds, shares its valences with four oxygen atoms equally (tetrahedrally) spaced around it. Aluminum also shares its valences with six oxygen atoms equally (octahedrally) spaced around it:

$$
\begin{array}{c}
\text{Al} \overset{\displaystyle O}{\underset{\displaystyle O}{\diagdown}} \\
\text{Al} \overset{\displaystyle O}{\underset{\displaystyle O}{\diagdown}}
\end{array} \quad \text{HYPOTHETICAL}
$$

```
                                                    O
                                                   /
           |                           |          O
           O                           O         /
           |                           |
  — O — Al — O —              — O — Al — O —
           |                           |
           O                       O   O
           |                      /    |
                                 O
```

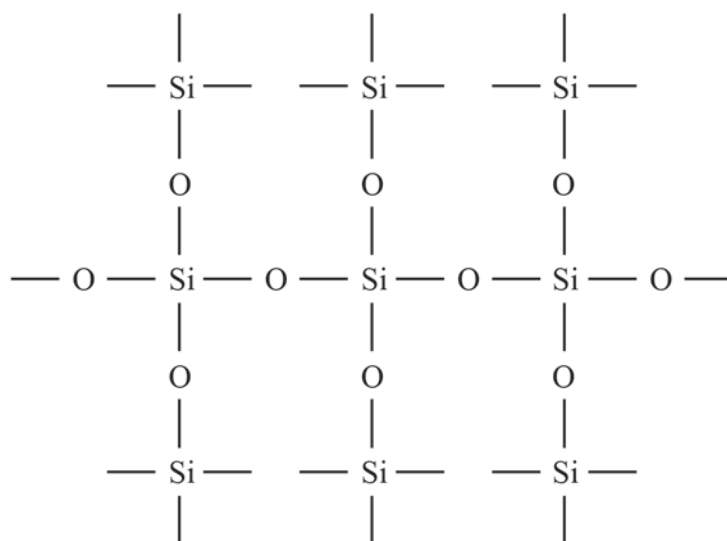TETRAHEDRAL   OCTAHEDRAL

If silica and alumina are combined, which type of aluminum-oxygen combination should be used? The silica-alumina catalyst gives no x-ray diffraction pattern that would permit a decision.
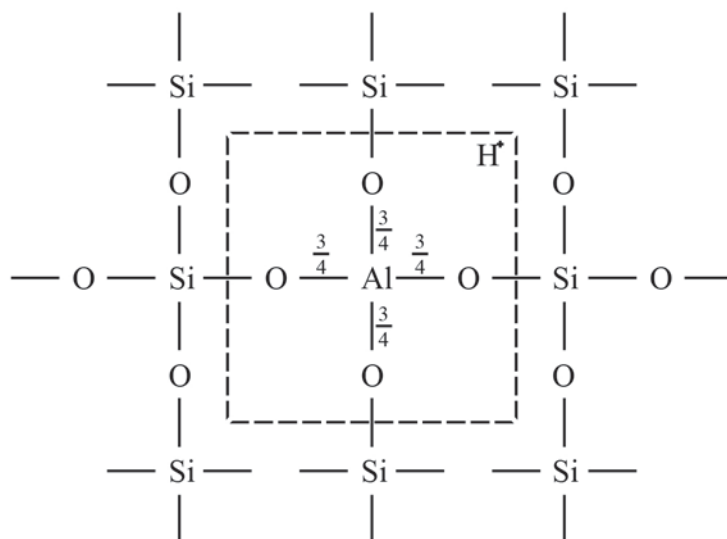
Therefore, the following assumptions were made:

1. The aluminum in the silica-alumina cracking catalyst that contributes to catalytic activity is tetrahedrally linked to four oxygen atoms.

2. A positive hydrogen ion is associated with tetrahedral aluminum in the cracking catalyst.

3. The catalytic activity of properly prepared silica-alumina masses is due to the acidic hydrogen ion associated with it.

Using assumption 1 the building blocks for the catalyst become tetrahedral silica and tetrahedral alumina. The following illustrates, in two dimensions, a three-dimensional network of silicon and oxygen:

```
      |            |            |
  —  Si  —     —  Si  —     —  Si  —
      |            |            |
      O            O            O
      |            |            |
  — O — Si — O — Si — O — Si — O —
      |            |            |
      O            O            O
      |            |            |
  —  Si  —     —  Si  —     —  Si  —
      |            |            |
```

Each line represents one valence unit. Each silicon atom has four such lines to satisfy its valence of four. Each oxygen atom has two such lines and its valence of two is satisfied. If the central silicon atom is removed and replaced with a tetrahedral aluminum atom, the result is:

```
      |               |              |
  —  Si  —        —  Si  —       —  Si  —
      |     ┌ ─ ─ ─ ─ ┼ ─ ─ ─ ─ ┐    |
      O     │         |      H⁺ │    O
      |     │        3/4        │    |
      |     │   3/4  |   3/4    │    |
  — O — Si ─┼─ O —— Al —— O ─┼─ Si — O —
      |     │        3/4        │    |
      |     │         |         │    |
      O     │         O         │    O
      |     │         |         │    |
  —  Si  —  └ ─ ─ ─ ─ ┼ ─ ─ ─ ─ ┘ —  Si  —
      |               |              |
```

It is known that the valence of aluminum is three. Each line attached to the aluminum atom represents three fourths of a valence unit. With four such lines the valence of aluminum is satisfied. The oxygen atoms share one valence with a silicon atom and three fourths of a valence with aluminum. Each oxygen atom has available

to it only one and three fourths valence units when its valence demands two. Each such oxygen atom is unsatisfied by one fourth of a valence unit, and there are four such oxygens for each aluminum atom. It follows that the AlO_4 part of the molecule is unsatisfied by a whole valence unit and, since oxygen is a negative element, this is a negative valence (Thomas, 1949).
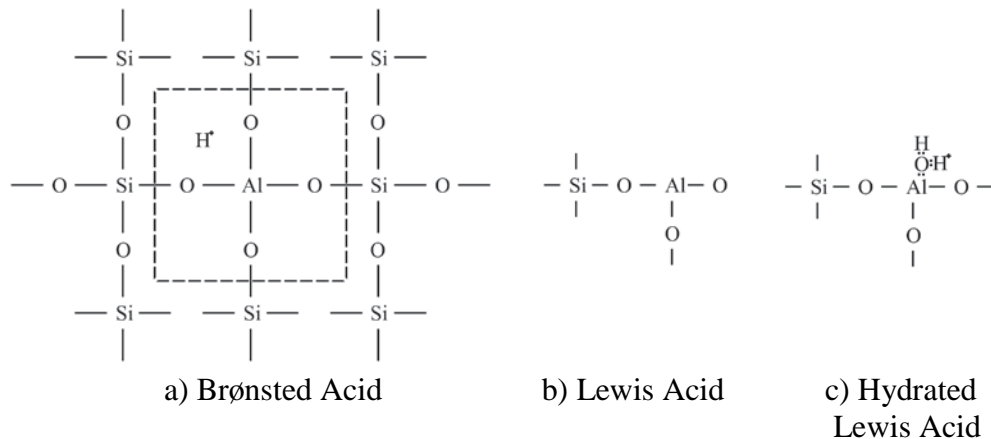

a) Brønsted Acid   b) Lewis Acid   c) Hydrated
                                                    Lewis Acid

Figure 1.1 Suggested cracking catalyst acid structures (Mapes & Eischens, 1954)

Aluminum silicate comes in three different forms: Andalusite, Sillimanite and Kyanite. They all have the chemical composition Al_2SiO_5, but are polymorphic having different crystal structures. All three forms occur under different temperatures and pressures so are rarely found in the same rock.

Some of the properties of Aluminum Silicate are:

- Lighter in weight
- Super white in color
- High degree of brightness
- Low plasticity
- Ease of dispersion
- Good oil absorption.

Aluminum Silicate minerals are used in bulk for some special applications such as making fine porcelains, paper coating and are used in industries like paints, plastics and fiberglass. It is also used in glassmaking as a refractory or catalyst due to its

insolubility. Pesticides containing aluminum silicate can replace organic pesticides. The substance called ultramarine Blue that is prepared by heating kaolin, sodium carbonate, sulfur is used to treat upset stomach medically.

Aluminum silicate has a remarkable use in paint industry as a filler and antisetting agent and in rubber industry; it is used as a partial reinforcing agent. It can be manufactured by processing of aluminum silicate minerals found naturally. It can also be prepared by precipitation that gives much better properties because of smaller particle sizes and higher strength value.

As aluminum silicate has very low moisture content, it improves electrical as well as mechanical properties of the composite thus making it fireproof. Various forms of the mineral are used to make gem stones because of their ability in strength retention even at high temperatures (Aluminum Silicate, 2011, http://www.tutorvista.com).

1.4 Sepiolite

The name Sepiolite was first used in 1847 by Glöcker and takes its origins from the Greek word for cuttlefish. The bones of cuttlefish are as light and porous as the mineral. Sepiolite occurs only with a fibrous habit. Sepiolite, formerly known as Meerschaum (sea froth), is a non-swelling, lightweight, porous clay with a large specific surface area. Unlike other clays, the individual particles of Sepiolite have a needle-like morphology (Sepiolite, 2011, www.ima-eu.org).

The clay mineral Sepiolite is a microcrystalline hydrated magnesium silicate of theoretical unit cell formula $Si_{12}O_{30}Mg_8(OH,F)_4(H_2O)_4.8H_2O$. (Figure 1.2) It exhibits a microfibrous morphology and a particle size in the 2-10 μm length range. Sepiolite shows an alternation of blocks and tunnels that grow up in the fiber direction Figure 1.3. The blocks are constituted by two layers of tetrahedral silica sandwiching a central magnesium oxide hydroxide layer, and the dimensions of the cross-section of tunnels are about 1.1x 0.4nm^2.
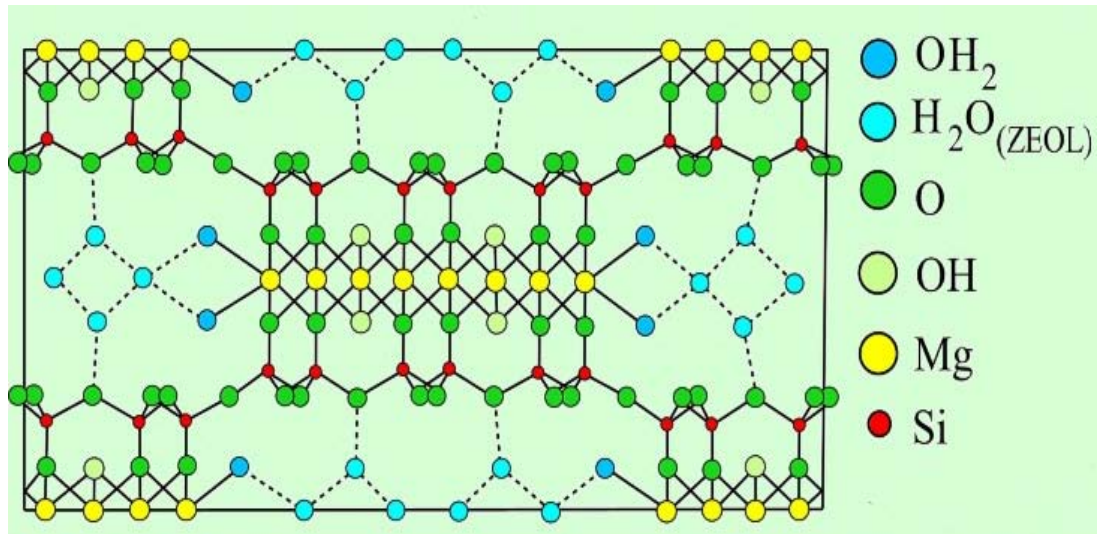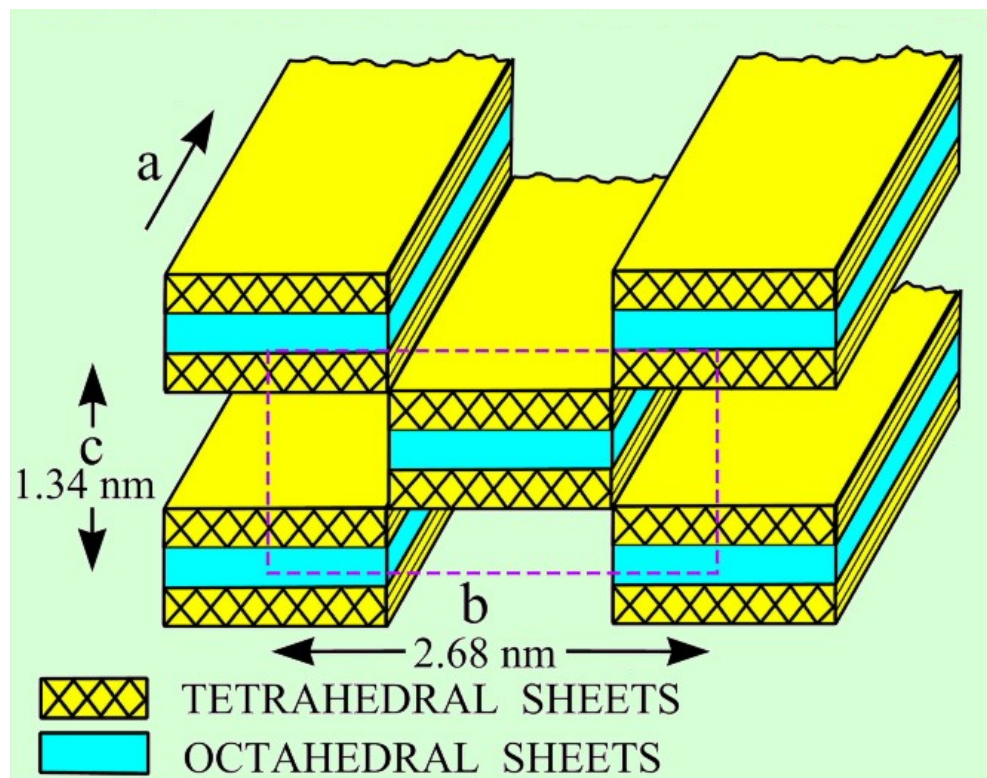
Figure 1.2 Structure of Sepiolite

Figure 1.3 Tunnels and blocks of Sepiolite mineral

The discontinuity of the silica sheets gives rise to the presence of silanol groups (Si-OH) at the edges of the channels, which are the tunnels opened to the external surface of the Sepiolite particles. Tunnels are filled with both the coordinated water molecules, which are bonded to the Mg^{2+} ions located at the edges of octahedral

sheets, and the zeolitic water, which is associated to the former by hydrogen bonding (Darder, Blanco, Aranda, Aznar, Bravo, & Hitzky, 2006). These tunnels are accessible to water molecules (zeolitic water) and also a variety of species, the only restriction being related to the dimensions of the guest species, the Sepiolite acting as a molecular sieve (Saavedra, Aranda, & Hitzky, 2004).

Sepiolite has been used for centuries because of their important colloidal and rheological properties and their capacity for sorption (Keith, 2000). The sorptive properties of Sepiolite classify it in a group of clays known collectively as fuller's earth. The term fuller's earth is a term used for highly absorbent and natural bleaching clays.

Sorptive properties of Sepiolite can be explained by three features:

- Oxygen ions associated with tetrahedral on ribbon edges may attract cations or molecules with dipoles to the mineral surface.
- H_2O molecules may be coordinated to magnesium ions at the edges of structural ribbons.
- Silanol (-SiOH) groups occur along the fiber axis of crystals.

Sorptive grade Sepiolite is used as decolorizing and clarifying agents, filter aids, floor adsorbents, animal litter, and pesticide carriers, components of the No-carbon copy papers, and catalysts and refining aids. Organically modified Sepiolite allows controlling the rheological behavior of different solvent-based systems as paints, greases, resins and inks enhancing their stability under a wide temperature range and making for easier application.

Sepiolite absorbs liquid spills and leaks keeping work and transit areas dry and safe. It is a non-flammable material with high liquid absorbing capacity, suitable mechanical strength of the granules even in wet conditions, and chemical inertness which avoids reaction with absorbed liquids. Sepiolite absorbs toxic and hazardous wastes in stabilization or in removal treatments. Sepiolite absorbs active chemicals,

as pesticides, remaining free-flowing and allowing an easy use and effective application of the product in the field.

The use of Sepiolite fillers improve processing, dimensional stability, mechanical strength and thermal resistance. Sepiolite allows controlling the rheological properties in heat application systems, improving fire resistance. It also improves binding of the components while increasing the fire resistance.

Sepiolite adsorbs excess humidity preventing condensation, corrosion, the proliferation of microorganisms and unpleasant odors. Then, Sepiolite can be use as cat and pet litters. The popularity of Sepiolite pet litters is due to its light weight, high liquid absorption and odor control characteristics. Sepiolite absorbs pet urine and has a dehydrating effect on solid faces which minimizes bad odors and inhibits bacteria proliferation. Sepiolite is registered in the EU as a technological additive for animal feed (E-562).

Sepiolite has numerous domestic applications such as moisture control, containment of accidental liquid spillages, and use in ashtrays to avoid smoke odor, control of liquid leakages and odors in dustbins, odor removal in refrigerators, etc (Sepiolite, 2011,www.ima-eu.org).

1.5 Bentonite

Bentonite is smectite clay formed from the alteration of siliceous, glass-rich volcanic rocks such as tuffs and ash deposits. The major mineral in bentonite is montmorillonite, a hydrated sodium, calcium, magnesium, aluminum silicate. The main constituent, which is the determinant factor in the clay's properties, is the clay mineral montmorillonite. The sodium, calcium, and magnesium cations are interchangeable giving the montmorillonite a high ion exchange capacity. Smectites are clay minerals, i.e. they consist of individual crystallites the majority of which are $< 2\mu m$ in largest dimension. Smectite crystallites themselves are three-layer clay

minerals. They consist of two tetrahedral layers and one octahedral layer (Bentonite, 2011, www.ima-eu.org).

Bentonite is a clay known as a 2/1 type aluminosilicate. Its crystalline structure presents an alumina octahedral between two tetrahedral layers of silica. The isomorphous substitution of Al^{3+} for Si^{4+} in the tetrahedral layer and Mg^{2+} for Al^{3+} in the octahedral layer results in a net negative surface charge on the clay. This charge imbalance in offset by exchangeable cations, denominated exchange cations (typically Na^+ and Ca^{2+}) to compensate the negative charges at the surface. The parallel layers in these structures are held together by weak electrostatic forces and can expand by penetration of polar species between the clay layers (Bouberka, Kacha, Kameche, Elmaleh, & Derriche, 2005). The extent of hydration produces inters crystalline swelling.

Depending on the nature of their genesis, bentonites contain a variety of accessory minerals in addition to montmorillonite. These minerals may include quartz, feldspar, calcite and gypsum. The presence of these minerals could impact the industrial value of the deposit, reducing or increasing its value depending on the application. Bentonite presents strong colloidal properties and its volume increases several times when coming into contact with water, creating a gelatinous and viscous fluid.

The special properties of bentonite (hydration, swelling, water absorption, viscosity, thixotropy) make it a valuable material for a wide range of uses and applications. Bentonite is subsequently dried (air and/or forced drying) to reach a moisture content of approximately 15%. According to the final application, bentonite is either sieved (granular form) or milled (into powder and super fine powder form) (Bentonite, 2011, www.ima-eu.org).
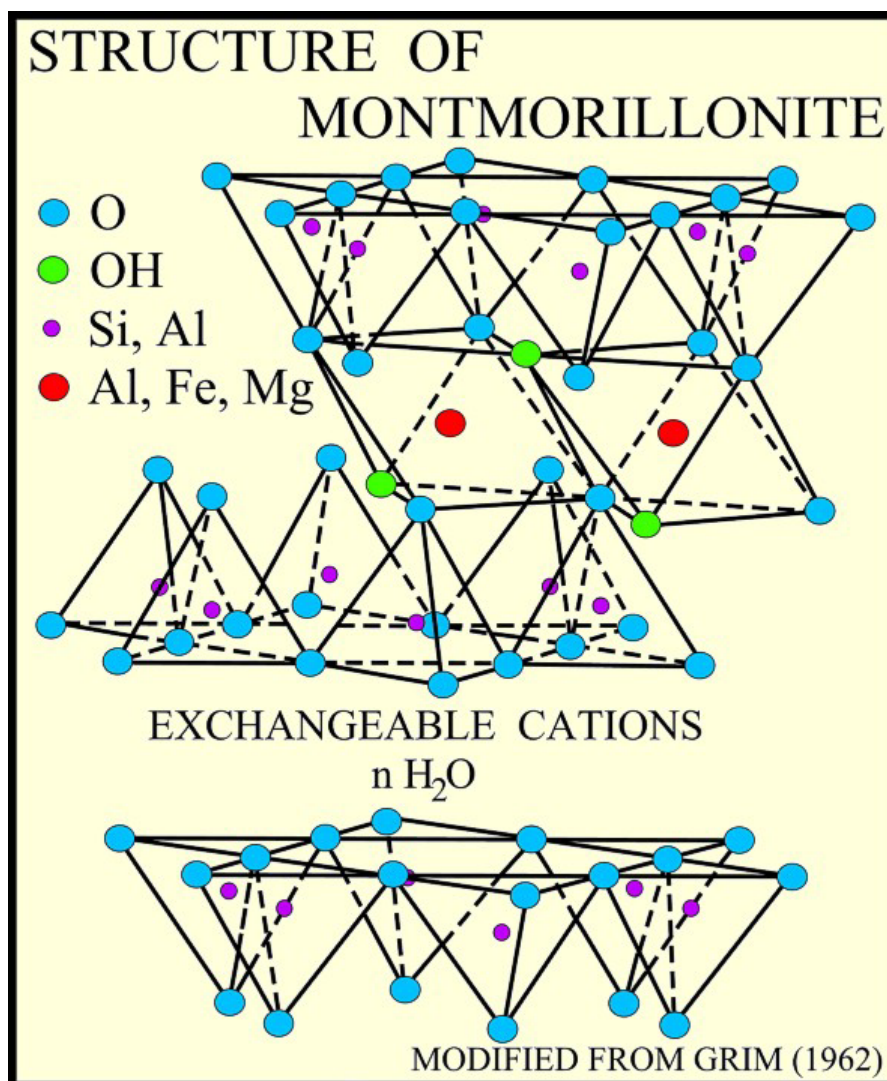
Figure 1.4 Structure of montmorillonite

Chemically modified clay catalysts find application in a diverse range of duties where acid catalysis is a key mechanism. Most particularly they are employed in the alkylation processes to produce fuel additives. Bentonite's adsorption / absorption properties are very useful for wastewater purification and its adsorption properties are appreciated for the finishing of indigo dying cloth and in dyes (lacquers for paints & wallpapers). Bentonite is utilized in the removal of impurities in oils where its adsorptive properties are crucial in the processing edible oils and fats (Soya/palm/ canola oil). Bentonite is used for cat litter due to its advantage of absorbing refuse by forming clumps (which can be easily removed) leaving the remaining product intact for further use.

In drinks such as beer, wine and mineral water and in products like sugar or honey, bentonite is used as a clarification agent. Another conventional use of bentonite is as a mud constituent for oil- and water- well drilling. Its role is mainly to seal the borehole walls, to remove drill cuttings and to lubricate the cutting head.

Bentonite is crucial to paper making, and also offers useful de-inking properties for paper recycling. In addition, acid activated bentonite is used as the active component in the manufacture of carbonless copy paper.

Bentonite is used as filler in pharmaceuticals and due to its absorption/adsorption functions, allows paste formation. Such applications include industrial protective creams, calamine lotion, wet compresses, and anti- irritants for eczema. In medicine, bentonite is used as an antidote in heavy metal poisoning. Personal care products such as mud packs, sunburn paint, baby and face powders, and face creams may all contain bentonite (Bentonite, 2011, www.ima-eu.org).

1.6 Purpose of the Study

One of the oldest and most intriguing chemical phenomena, catalysis, has become indispensable for living over the past three centuries. People would even not exist without catalysis, since the body is a complex catalytic factory using very efficient biocatalytic reactions. Moreover, about 70% of all industrial processes make use of catalysts, while approximately 90% of produced chemicals are prepared with the aid of catalysts. A few examples where to encounter catalysis, or products made by catalysts, in daily life, are: exhaust catalysis, batteries, detergents, gasoline, food (beer, wine, and cheese), polymers (and products made out of them) (Catalytic Processes and Materials, http://www.utwente.nl/tnw/cpm/, 2011).

The concept of surface acidity is especially important in various catalytic reactions. The catalytic activity of acid solids is not only related to the surface concentration of acid sites, but also depends on their nature (i. e. Brønsted or Lewis type) and strength (Selli & Forni, 1999). The well-definition of the acidic properties

of a solid surface covers the quantitative determination of the acidity, the nature of the acid sites (Lewis or Brønsted acid centers) and also the reactivity of these acidic centers. The results of acidity investigations can be defined in terms of Hammett acidity functions (Yurdakoç, Akçay, Tonbul, & Yurdakoç, 1999).

The aim of this study is to determinate the surface acidity of various SiO_2-Al_2O_3, Sepiolite and Bentonite catalysts. The surface acidities of various SiO_2-Al_2O_3, Sepiolite and Bentonite catalysts will be examined by way of n-butyl amine titration technique with Hammett indicators in nonaqueous solvents such as benzene, back titration with $NaHCO_3$, Na_2CO_3 and $NaOH$ bases in aqueous solution. Surface functional groups of various SiO_2-Al_2O_3, Sepiolite and Bentonite catalysts will also examined. Furthermore, the Brønsted and Lewis acid sites of the catalysts will be investigated after the adsorption of pyridine in gas phase by FTIR spectroscopic method of analysis which is very important in catalysis as far as surface structures concerned.

MATERIALS AND METHODS

2.1 Materials

The silica-alumina (SIRAL) samples used in this work were the obtained from CONDEA AG-Germany, now (SASOL). The compositions, surface areas and the pore size distribution of the samples are given in Table 2.1. Bentonite and Sepiolite were obtained from Enez/Edirne and Eskişehir, respectively. The properties of the natural clays are summarized in Table 2.2 and 2.3. BET specific surface area of bentonite and sepiolite were determined as 77 and 292 m^2/g respectively by adsorption of N_2 at 77K with Quantachrome Autosorb Automated Gas Sorption System. Characterization data of the samples are given in Table 2.4.

Table 2.1 Characterization data of silica-alumina samples

Sample	SiO_2 content %	Al_2O_3 content %	BET Area m^2g^{-1}	density gmL^{-1}	Particle size distribution (%)		
					<25μ	<45μ	<90μ
Siral 5	4.5	95.5	380	0.53	20.7	49.1	90.0
Siral 20	21.8	78.2	428	0.38	36.5	69.9	99.9
Siral 30	28.1	71.9	467	0.34	26.9	52.1	94.0
Siral 40	39.7	60.3	506	0.33	26.3	52.2	94.1
Siral 80	78.3	21.7	224	0.54	73.3	96.2	98.7

Table 2.2 Chemical composition of Bentonite

Component	%
SiO_2	57.78
Al_2O_3	19.24
Fe_2O_3	3.58
MgO	2.13
CaO	4.21
Na_2O	2.73
K_2O	1.35
Sulphate	-
Ignition Loss	7.48

Table 2.3 Chemical composition of Sepiolite

Component	%
SiO_2	48.00
Al_2O_3	0.50
Fe_2O_3	0.40
MgO	24.00
CaO	4.00
Na_2O	0.02
K_2O	0.03
Sulphate	0.02
Ignition Loss	23.03

Table 2.4 The properties of Bentonite and Sepiolite

Sample	CEC (meg/100g clay)	BET Specific Surface Area (m^2/g)	D_{001} (Å)	Total Pore Volume (cm^3/g)	Average Pore Diameter (Å)
Bentonite	97	76.84	7.63	0.203	105.8
Sepiolite	82	292	12.56	0.575	80.04

Other chemicals were purchased Merck and Fluka in reagent grades as follows; NaHCO$_3$ (Merck No. 6329), Na$_2$CO$_3$ (Merck No. 6398), NaOH (Merck No. 6462), Benzene (Fluka No. 12560), n-butyl amine (Merck No.801539), Neutral red (Merck No. 1369), Methyl red (Merck No. 6076), 4-nitroaniline (Merck No. 822292), crystal violet (Merck No. 1408), 2-nitroaniline (Merck No. 820881), 4-chloro-2-nitroaniline (Merck No. 802625), 2,4-dinitroaniline (Merck No. 803248), anthraquinone (Merck No. 800465). They were all used directly without further purification.

2.2 Acid Strength Measurements

All samples were freshly dried at 110 ºC for 2 h. Color tests were made by transferring 0.1 g of dried, powdered solid to a test tube, adding 3 mL benzene and a 0.1 % solution of indicator in benzene (three drops in the case of all indicators). The solutions were shaken at 140 rpm and at 323 K in a temperature controlled shaking water bath (Memmert) for 24 h to reach equilibrium under experimental conditions. From the results of such tests, it was easy to decide whether the solid under study was basic to all indicators, acid to all indicators, or had an H$_O$ lying between two adjacent indicator pKa's. Samples were freshly dried at 393 K before carrying out the indicator tests, and were subjected to color immediately after drying, or if this was not convenient, were stored in screw cap test tubes in a desiccator until color tests were performed. Since water is a base, the effect of water adsorption changed the color intensities of the adsorbed indicators or caused a shift to lower acid strengths.

2.3 Quantitative determination of acid sites

The amount of acid sites on the samples can be measured by amine titration immediately after determination of acid strength by above method. The method consists of titration of the sample suspended in benzene with n-butyl amine, using an indicator. The 0.1 N n-butyl amine solution was prepared by weighing 1.0 mL of n-butyl amine in a 100 mL volumetric flask and making up the volume using dried benzene. The procedure was as follows: 0.2g of dried sample was transferred to a 50 mL screw-cap Erlenmeyer flask. Nine millil iters of dry benzene and 3 mL of

indicator solution in benzene were added to the sample suspension. The tightly capped sample was then equilibrated in a rotator at least twenty-four hours at room temperature. Then, enough 0.1N n-butyl amine in benzene was added from a 2 mL burette to the sample so as to bracket the expected titer by the appropriate number of millimoles of n-butyl amine per gram of sample. The titration was then continued using smaller stepwise increases in n-butyl amine content until the end point.

2.4 Determination of the Acidity in Aqueous Solution with Bases by the back-titration Method

Dried samples of each 0.2 g were transferred to a 50 mL screw-cap Erlenmeyer flasks. 25 mL of NaOH, Na_2CO_3, $NaHCO_3$ solutions were added to the sample suspensions. The tightly capped samples were shaken at 140 rpm and at 80ºC for 1h and then further at 25 ºC for 24 h in a temperature controlled shaking water bath (Memmert). After 2 h, the samples were taken and centrifuged at 4000 rpm for 5 min. 10 mL of each of samples are titrated with 0.0945 N HCl solution previously standardized with Na_2CO_3 solution. The indicators for the titrants are following; Na_2CO_3; methyl orange; NaOH: methyl orange; $NaHCO_3$: methyl red.

2.5 Determination of Point of Zero Charge (pH_{pzc}) of the samples

The determination of pH_{pzc} of samples was carried out by pH titration procedures. 25 mL of NaCl (0.01 M) solution was poured into several Erlenmeyer flasks. The pH of solution within each flask was adjusted to a value between 2 and 7 by addition of HCl (0.1 M) or NaOH (0.1 M) solution. Then 0.075g of solid sample was added to the flasks. The solutions were shaken at 140 rpm and at 298 K in a temperature controlled shaking water bath (Memmert) for 48 h to reach equilibrium under experimental conditions. Then the final pH was measured. The pH_{pzc} is defined as the point where the curve pH_{final} vs $pH_{initial}$ crosses the line $pH_{final} = pH_{initial}$

2.6 Fourier Transform Infrared (FTIR) Spectra of the Samples

IR measurements were performed with self-supporting pressed discs contained in a cell with NaCl windows, which allowed discs to be heated under vacuum or in the presence of pyridine. IR spectra were recorded in situ at room or at elevated temperatures by a Perkin-Elmer FTIR spectrophotometer Spectrum BX-II, equipped with a conventional evacuation-gas manipulation ramp (10^{-3} Pa).

The FTIR instrument was typically operated at a resolution of 2 cm^{-1}, collecting 50 scans per spectrum. All the samples were subjected to a standard pretreatment involving heat treatment at 573 K in vacuo for 1 h. After adsorption studies, desorption experiments were also done at elevated temperatures for 10 min. The quantitative analysis of the pyridine adsorption was carried out after initial, 15min., 30 min and at 373 K adsorption procedures and followed by successive evacuations (desorption) at elevated temperatures until 573 K for 10 mins for all of the temperature periods at a pressure of 10^{-3} Pa.

CHAPTER THREE

RESULTS AND DISCUSSION

3.1 Acid Strength Measurements

Acidic strengths of samples are given in Table 3.1, respectively. The limits of the H_O of samples were established by observing the color of the adsorbed form of the Hammett indicators. As can be seen from Table 3.1, all the samples had an acid strength of $H_O \leq +4.8$ which means that the sample with an $H_O < +1.1$ gave acid colors with all Hammett indicators.

Table 3.1 Distribution of the acidic strength with Hammett indicators

Indicator	Siral 5	Siral 20	Siral 30	Siral 40	Siral 80	Sepiolite	Bentonite
Neutral red pKa= +6.8	+	+	+	+	+	+	+
Methyl red pKa= +4.8	+	+	+	+	+	+	+
4-Nitroaniline pKa=+1.1	−	−	−	−	−	−	−
Crystal violet pKa=+0.8	−	−	−	−	−	−	−
2-Nitroaniline $pK_a = -0.2$	−	−	−	−	−	−	−
4-chloro-2-nitroaniline $pK_a = - 0.9$	−	−	−	−	−	−	−
2,4-dinitroaniline $pK_a = - 4.4$	−	−	−	−	−	−	−
Anthraquinone pKa=-8.2	−	−	−	−	−	−	−

3.2 Quantitative determination of acid sites

The amounts of acid in the samples are given in Table 3.2, respectively. It can also be seen from Table 3.2 that the calculated total amounts of acids in the samples with the increase in SiO_2 content up to Siral 40 and then decreased sharply in the case of Siral 80 with approximately 80% of SiO_2. The maximum amount of acidity was observed in the case of Siral 40 as 0.8 mmole/g. We assumed that 20 $\breve{A}^2$ is the area of an acid site in the case of the silica-alumina catalysts (Benesi, 1957).

Table 3.2 The amount of acids as mmole g^{-1} which was calculated from the n-butyl amine titration

Indicator	Siral 5	Siral 20	Siral 30	Siral 40	Siral 80	Sepiolite	Bentonite
Neutral red pKa= +6.8	0.17	0.20	0.24	0.28	0.45	0.57	0.26
Methyl red pKa= +4.8	0.30	0.40	0.47	0.55	0.36	0.57	1.50
4-Nitroaniline pKa=+1.1	–	–	–	–	–	–	–
Crystal violet pKa=+0.8	–	–	–	–	–	–	–
2-Nitroaniline pK_a = -0.2	–	–	–	–	–	–	–
4-chloro-2-nitroaniline pK_a = - 0.9	–	–	–	–	–	–	–
2,4-dinitroaniline pK_a = - 4.4	–	–	–	–	–	–	–
Anthraquinone pKa=-8.2	–	–	–	–	–	–	–

The binary oxide of SiO_2-Al_2O_3 develops much stronger acids than those of individual oxides upon the evacuation under heating. Their acid strength is higher at smaller contents of Al_2O_3. Without the evacuation, the presence has been reported of 0.25 mmole g^{-1} of acids of $H_O \leq 1.5$ on the catalyst which contained 15 wt% of Al_2O_3, and 0.57 mmole g^{-1} of acid ($H_O \leq 3.3$) (Tanabe, 1970). Bentonite is more acidic than Sepiolite because of more SiO_2 content.

The experiments were performed at room temperature after drying the samples at 393 K as a standard pretreatment procedure. It should perhaps be pointed out at this stage that the acidic properties of silica-alumina to a large extent depend upon the method of preparation, the proportion of alumina, the temperature of dehydration, and the method by which the acidity is assessed. Changes in these acidic properties due to both grinding and steam heating have also been reported (Tanabe, 1970).

3.3 Determination of the Acidity in Aqueous Solution with Bases by the back-titration method

Surface functional groups on samples were determined by Boehm's titration (Boehm, 1994; Toles et al., 1999). In this method, certain titrable surface functional groups on the samples can be determined and quantify the amount of various types of oxygenated groups.

Initially, acid sites on surface are neutralized by excess $NaHCO_3$, Na_2CO_3, NaOH base solutions in aqueous solution. Then the remaining bases are back- titrated with a standardized HCl solution. The numbers of acidic sites of various types were calculated using the assumptions that NaOH neutralizes carboxylic, phenolic, and lactonic groups, Na_2CO_3 neutralizes carboxylic and lactonic groups, and $NaHCO_3$ neutralizes only carboxylic groups (Boehm, 2008). Boehm titration results were calculated as meq/g by the Equation 3.1.

$$meq/g = \{(V_{base} \times N_{base}) - [S_{acid} \times (V_{base}/V_{titrant}) \times N_{acid}]\}/m \qquad (3.1)$$

V is the volume of the solution, S is the volume of the titrant and N is the concentrations of the solutions, m is mass of the sample in g. Results have been given for each samples at Table 3.3.

Table 3.3 Determine the acidity in aqueous solution with bases by the back-titration (meq g^{-1})

	NaHCO$_3$	Na$_2$CO$_3$	NaOH
Siral 5	0.13	-2.32	0.86
Siral 20	0.30	-1.87	1.21
Siral 30	0.46	-1.99	1.80
Siral 40	0.52	-2.43	1.45
Siral 80	0.46	-1.76	1.21
Sepiolite	0.46	-3.75	-1.28
Bentonite	-1.76	-3.09	-0.39

Results have been showed that any acidic and basic group have not been found on the surface of samples.

3.4 Determination of the Point of Zero Charge

The point of zero charges of adsorbents (pH$_{pzc}$) is a point where an adsorbent have zero potential charge on its surface. At this point on the surface of the adsorbent there is no positive or negative charge density. The presence of H$^+$ or OH$^-$ ions in solutions may change the potential surface charges of adsorbents. If the pH of solution is above its pH$_{pzc}$ the surface functional groups on adsorbents will be protonated by the excess H$^+$ ions; on the contrary if it is below its pH$_{pzc}$, the surface functional groups will be deprotonated by the OH$^-$ ions presence in the solution (Putra, Pranowo, Sunarso, Indraswati, & Ismadji, 2009). If the pH value of the solution is lower than the pH$_{pzc}$ adsorbent surface cannot interact with acidic groups (positively charged), because there is a competition from H$^+$ ions for surface complexation sites of adsorbent and the surface have net positive charged (Kubilay, Gürkan, Savran, & Sahan, 2007). Similarly if the pH value of the solution is higher

than pH_{pzc} the adsorbent surface cannot interact with basic groups (negatively charged) because of the repulsion between the same charged groups.

Figure 3.1-3.7 indicate that the point of zero charge of the Siral 5, Siral 20, Siral 30, Siral 40, Siral 80, Sepiolite and Bentonite respectively. Results have been shown in Table 3.4.
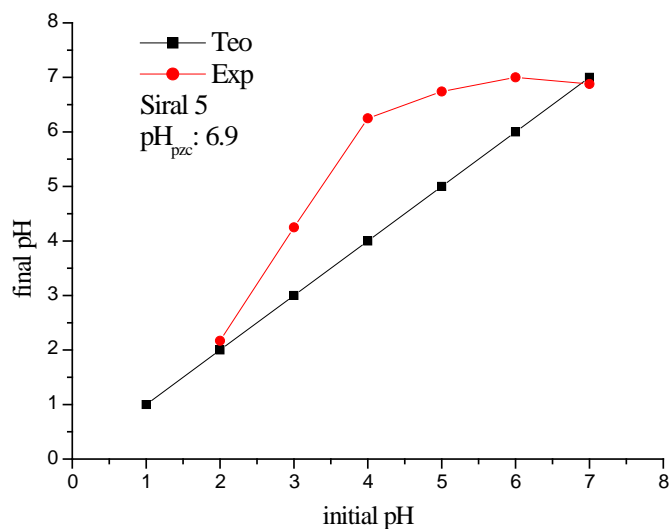

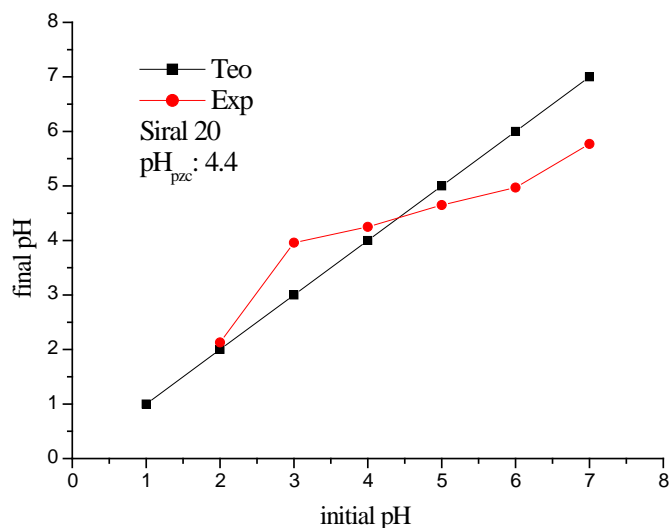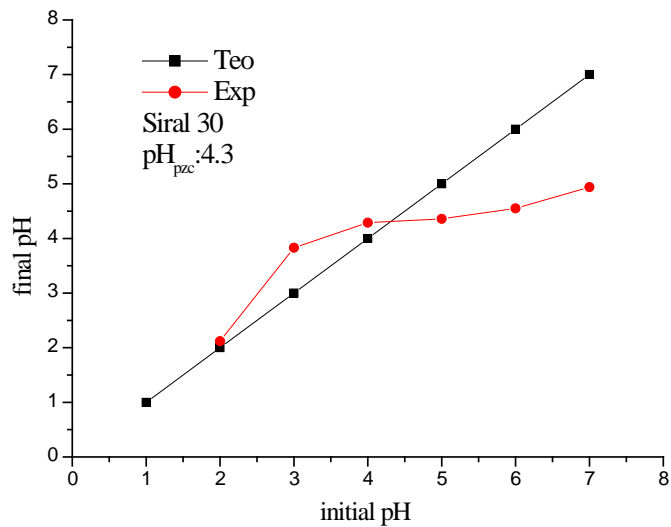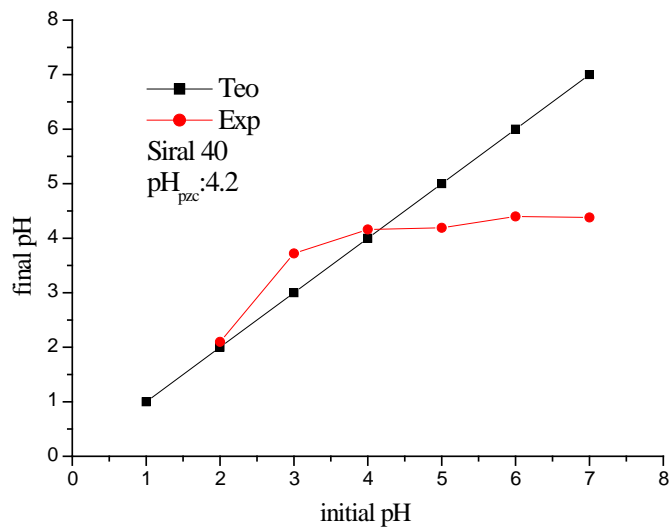Figure 3.1 Point of zero charge of Siral 5, m=0.075g, V=25mL.

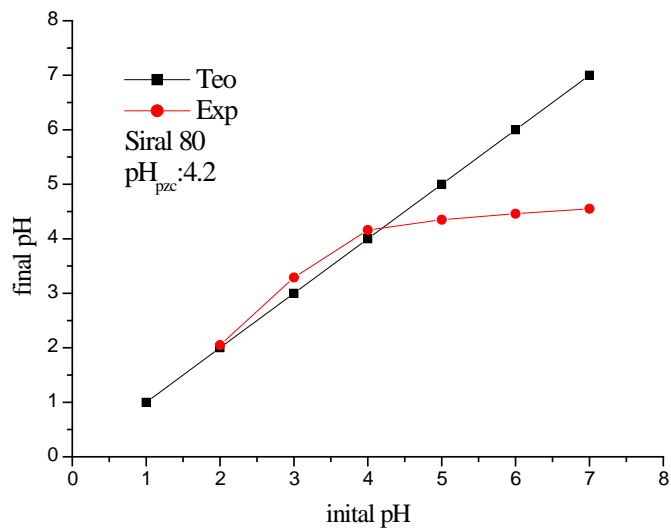Figure 3.2 Point of zero charge of Siral 20, m=0.075g, V=25mL.

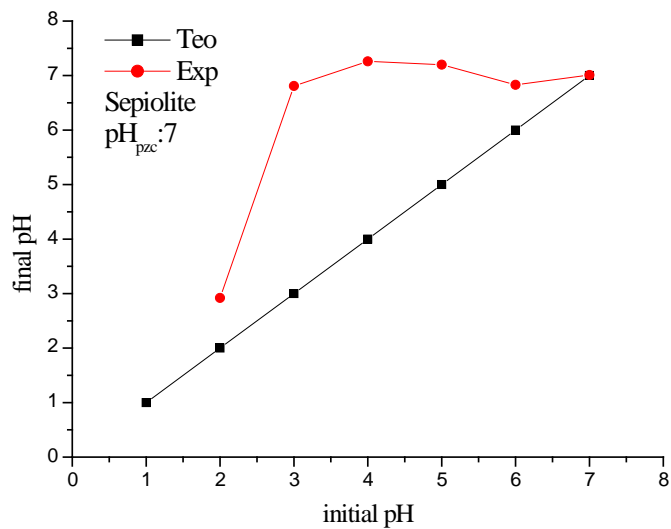Figure 3.3 Point of zero charge of Siral 30, m=0.075g, V=25mL.

Figure 3.4 Point of zero charge of Siral 40, m=0.075g, V=25mL.

Figure 3.5 Point of zero charge of Siral 80, m=0.075g, V=25mL.
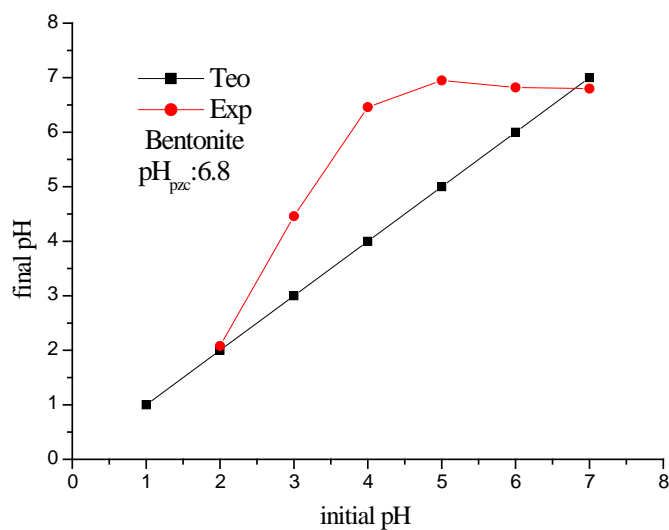

Figure 3.6 Point of zero charge of Sepiolite, m=0.075g, V=25mL.

Figure 3.7 Point of zero charge of Bentonite, m=0.075g, V=25mL.

Table 3.4 Point of zero charge of the samples

Sample	Point of Zero Charge pH
Siral 5	6.9
Siral 20	4.4
Siral 30	4.3
Siral 40	4.2
Siral 80	4.2
Sepiolite	7
Bentonite	6.8

The points of zero charge for Siral 5, Sepiolite and Bentonite ranged from 6.8 to 7. Points of the zero charge of Siral 5, Sepiolite and Bentonite explain that the surface of Siral 5, Sepiolite and Bentonite have not been included any positive or negative charge. The points of zero charge for Siral 20, Siral 30, Siral 40 and Siral 80 were ranged from 4.2 to 4.4. Points of the zero charge of Siral 20, Siral 30, Siral 40 and Siral 80 explain that the surface of Siral 20, Siral 30, Siral 40 and Siral 80 have been included positive charge.

The surface acidity or basicity gives the surface charge to any structure. The results of the surface functional groups, and point of zero charge analysis have been supported each other.

3.5 Fourier Transform Infrared (FTIR) Spectra of the Samples

IR measurements were performed with self-supporting pressed discs contained in a cell with NaCl windows, which allowed discs to be heated under vacuum or in the presence of pyridine. IR spectra were recorded in situ at room or elevated temperatures by a Perkin-Elmer FTIR spectrophotometer Spectrum BX-II, equipped with a conventional evacuation-gas manipulation ramp (10^{-3} Pa).

The FTIR instrument was typically operated at a resolution of $2 cm^{-1}$, collecting 50 scans per spectrum. All the samples were subjected to a standard pretreatment involving heating at 573 K in vacuo for 1h. After adsorption studies, desorption experiments were also done at elevated temperatures for 10 min.

The quantitative analysis of the pyridine adsorption was carried out after initial, 15min., 30 min and at 373 K adsorption procedures and followed by successive evacuations (desorption) at elevated temperatures until 573 K for 10 mins for all of the temperature periods at a pressure of 10^{-3} Pa. The bands at 1490 and 1450 cm^{-1} were employed for the determination of Brønsted and Lewis acid sites respectively. The extinction coefficients (ε) of these bands are available in the literature (Hughes & White, 1967; Emeis, 1993; Makarova, Karim, & Dwyer, 1995; Khabtou, Chevreau, & Lavalley, 1994; Datka, Turek, Jehng, & Wachs, 1992; Turek, Wachs, & DeCanio, 1992; Barzetti, Selli, Moscotti, & Forni, 1996; Datka, Gil, & Kubacka, 1995; Rajagopal, Marzari, & Miranda,1995). The concentration of Brønsted and Lewis acid sites referenced to unit weight of dry sample [q_H (mmole/g)] was obtained according to the equation 3.2 (Barzetti, Selli, Moscotti, & Forni, 1996).

$$q_H = \frac{A\pi R^2}{w\varepsilon}$$
(Eq. 3.2)

Where R(cm) is the radius of the catalyst wafer and w(g) is the weight of the dry sample. A (absorbance) values were evaluated from the difference spectra relative to all samples after baseline correction. ε values relative to the absorption bands at 1490 cm^{-1} (Brønsted sites, ε_B) and at 1450 cm^{-1} (Lewis sites, ε_L) were used as 1.67 and 2.22 cm$^2\mu$mol^{-1} which were reported in the literature (Emeis, 1993). The calculated values according to the equation above are given in Table 3.5. IR band assignments of difference spectra of pyridine adsorbed onto acidic catalysts are given in Table 3.6 (Barzetti et al., 1996). IR band assignments of difference spectra of pyridine adsorbed onto alumina are given in Table 3.7(Parry, 1963; Kiviat & Petrakis, 1973; Knözinger, 1976; Kiselev & Uvarov, 1967). The scheme for FTIR measurements are given in Figure 3.8.

Table 3.5 The concentration of Brønsted and Lewis acid sites calculated from the pyridine adsorption data

Sample	$q_H{}^L$ (mmol/g)	$q_H{}^B + q_H{}^L$ (mmol/g)
Siral 5	1.230	2.553
Siral 20	1.319	4.078
Siral 30	3.156	4.857
Siral 40	2.877	4.904
Siral 80	3.087	4.243
Sepiolite	0.525	2.219
Bentonite	0.196	0.575

Table 3.6 IR band assignments of difference spectra of pyridine adsorbed onto acidic catalysts

Absorption band cm^{-1}	Absorbed species	Acid site	Reference
1635	pyridinium ion	Brønsted	Barzetti et al. ,1996
1621	pyridine	Lewis	Barzetti et al. ,1996
1576	pyridine	Lewis	Barzetti et al. ,1996
1545	pyridinium ion	Brønsted	Parry, 1963
1495	C-H bending of aliphatics		Jacobs & Uytterhoeven,1972
1490	pyridinium ion+ pyridine	Lewis	Yashima & Hara, 1972
1462	C-H bending of aliphatics		Jacobs & Uytterhoeven,1972
1455	Pyridine	Lewis	Parry, 1963
1397	pyridinium ion	Brønsted	Barzetti et al. ,1996

Table 3.7 IR band assignments of difference spectra of pyridine adsorbed onto alumina

Sample	Pretreatment Temperature(°C)	Desorption Temperature(°C)	19b Mode (cm^{-1})			8a Mode (cm^{-1})			
η-Al$_2$O$_3$	450	25	1450			1583	1600	1621	
		150-230		1453	1457			1622	1632
		325-565			1458				
η-Al$_2$O$_3$	500	150		1453				1618	1625
		500			1457				1625
η-Al$_2$O$_3$	650	25	1445			1597	1610		1620
		100-200		1450-	1455			1617	1623
		300			1455				1623
γ-Al$_2$O$_3$	650	25		---			1615		
		250						1620	
γ-Al$_2$O$_3$	500	150		1453	1456				1623
		500							1623
γ-Al$_2$O$_3$	500	100			1457			1615	
δ-Al$_2$O$_3$	150-800	25		1444	1449	1589	1606		
		125					1606	1620	
		350						1620	
δ-Al$_2$O$_3$	300-800	25-200		1449			1614	1617	
		250		1449				1617	
		300-400			1452	1624			

The spectra of pyridine adsorbed on Siral 5, Siral 20, Siral 30, Siral 40, Siral 80, Sepiolite and Bentonite are shown in Figures 3.9-3.15, respectively. In Figures 3.9-3.15 we observed the bands at 1634, 1576 and 1394 cm^{-1} which are ascribed to as pyridinium ion (Brønsted species) and the bands at 1621, 1576, 1490 and 1456 cm^{-1} which are ascribed to as pyridine (Lewis species). The band at 1490 cm^{-1} is consistent with both Brønsted and Lewis acid sites, which can be seen in Table 1.6. Therefore, the calculated values of Brønsted acid sites from the band at 1490 cm^{-1} do not reflect the pure Brønsted acid sites. The presence of physically adsorbed pyridine apparently held on the surface by hydrogen-bonding interaction with surface OH groups is indicated by the detection of the characteristic 1595 and 1614 cm^{-1} bands. The data also indicate that some molecular water was very strongly adsorbed by the samples, since evacuation at 573 K did not completely remove it from the surface.
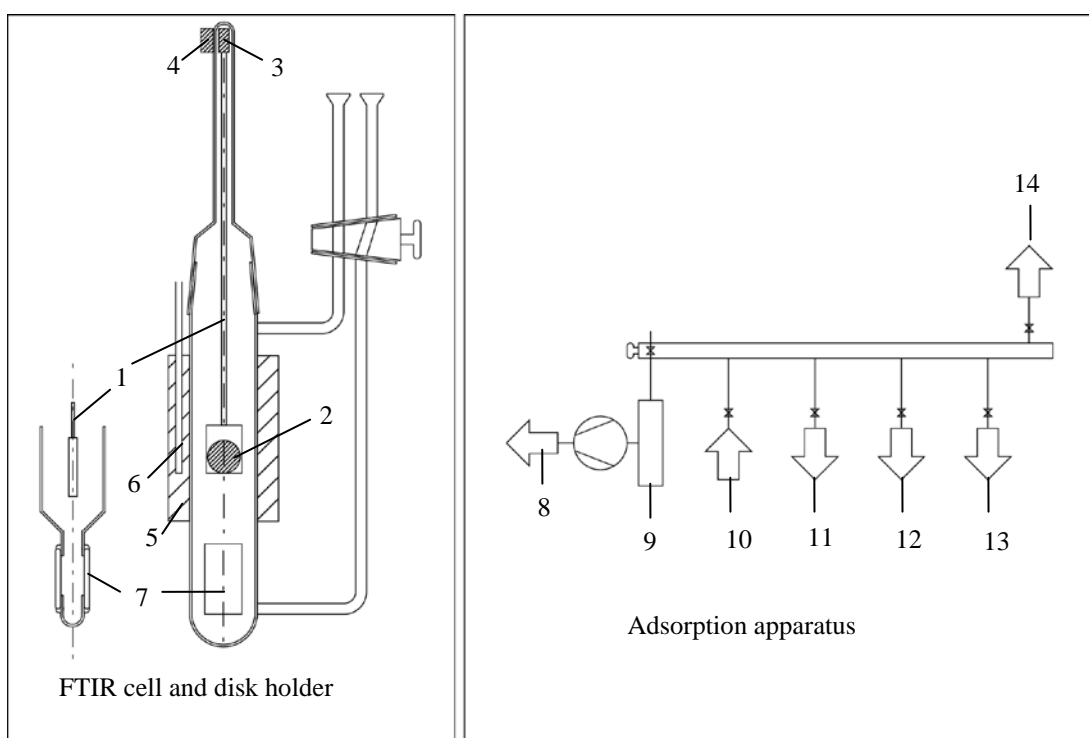

Figure 3.8 Scheme for FTIR measurements: 1) glass rod; 2) sample and its holder; 3) iron core; 4) movable magnet; 5) heating tape; 6) thermocouple; 7) NaCl windows; 8) vacuum pumps; 9) liquid-nitrogen trap; 10) IR cell gas inlet; 11) IR cell gas output; 12) gas inlet; 13) pyridine inlet; 14) vacuum gages

The FTIR spectra of pyridine adsorbed on Siral 5 is shown in Figure 3.9, respectively. In Figure 3.9, after evacuation at successively higher temperatures, it was observed that the band at 1436 cm^{-1} was gradually narrowed, its intensity decreased, and the band also shifted to 1445 cm^{-1}. The intensity of the band at 1489 cm^{-1} which was ascribed to the characteristic band as pyridinium ion and pyridine (Lewis species) decreased gradually after evacuation at 298 K. In Figure 3.9d, the bands at 1482, 1635 and 1540 cm^{-1} were ascribed to the characteristic band as BPy species. On the other hand, the bands at 1436 and 1622 cm^{-1} were ascribed to the characteristic band as LPy species. It was also observed that LPy species were more than BPy species on Siral 5.

The FTIR spectra of pyridine adsorbed on Siral 20 is shown in Figure 3.10, respectively. In Figure 3.10, after evacuation at successively higher temperatures, it was observed that the band at 1436 cm^{-1} was gradually narrowed, its intensity decreased, and the band shifted to 1444 cm^{-1}. In Figure 3.10d the bands at 1634, 1540, 1488 and 1394 cm^{-1} were ascribed to the characteristic band as BPy species. On the other hand, the bands at 1437 and 1622 cm^{-1} were ascribed to the characteristic band as LPy species. The band at 1557 cm^{-1} was gradually narrowed, its intensity decreased after evacuation at successively higher temperatures. After desorption at 573 K it was observed the band at 1490 cm^{-1} which was ascribed to the characteristic band as pyridinium ion and pyridine (Lewis species).

The FTIR spectra of pyridine adsorbed on Siral 30 is shown in Figure 3.11, respectively. In Figure 3.11, after evacuation at successively higher temperatures, it was observed that the band at 1441 cm^{-1} was gradually narrowed, its intensity decreased, and the band shifted to 1444 cm^{-1}. The intensity of the band at 1490 cm^{-1} decreased gradually after desorption at 298 K and then largely disappeared at 573 K. In Figure 3.11d the bands at 1633, 1490, 1394 cm^{-1} were ascribed to the characteristic band as BPy species. On the other hand, the bands at cm^{-1} 1613, 1591 and 1441 cm^{-1} were ascribed to the characteristic band as LPy species.

The FTIR spectra of pyridine adsorbed on Siral 40 is shown in Figure 3.12, respectively. In Figure 3.12, after evacuation at successively higher temperatures, it was observed that the band at 1444 cm^{-1} was gradually narrowed, its intensity decreased, and the band shifted to 1456 cm^{-1}. In Figure 3.12d the bands at 1634, 1489 and 1394 cm^{-1} were ascribed to the characteristic band as BPy species. On the other hand, the bands at 1622, 1444 and 1590 cm^{-1} were ascribed to the characteristic band as LPy species. After desorption at 573 K it was observed that the band at 1490 cm^{-1} which was ascribed to the characteristic band as pyridinium ion and pyridine (Lewis species).

The FTIR spectra of pyridine adsorbed on Siral 80 is shown in Figure 3.13, respectively. In Figure 3.13, after evacuation at successively higher temperatures, it was observed that the band at 1445 cm^{-1} was gradually narrowed, its intensity decreased. After desorption at 473 and 573 K it was observed the band at 1454cm^{-1} which was ascribed to the characteristic band as pyridine species (Lewis sites). In Figure 3.13d the band at 1490 cm^{-1} was ascribed to the characteristic band as BPy species. On the other hand, the bands at 1443 and 1591 cm^{-1} were ascribed to the characteristic band as LPy species. After desorption at 573 K it was observed that the band at 1490 cm^{-1} which was ascribed to the characteristic band as pyridinium ion and pyridine (Lewis species). It was observed that the band at 1622 cm^{-1} which was ascribed to the characteristic band as pyridine (Lewis species) at 573 K.

The FTIR spectra of pyridine adsorbed on Sepiolite is shown in Figure 3.14, respectively. In Figure 3.14, after evacuation at successively higher temperatures, it was observed that the band at 1557 cm^{-1} was gradually narrowed, its intensity decreased. After desorption at 298, 373, 473 and 573 K, it was observed that the band at 1455 cm^{-1} which was ascribed to as the characteristic band pyridine species (Lewis sites). In Figure 3.14d the bands at 1634, 1489 and 1394 cm^{-1} were ascribed to the characteristic band as BPy species. On the other hand, the bands at 1622, 1444 and 1590 cm^{-1} were ascribed to the characteristic band as LPy species. As can be seen also in Figure 3.14e, after desorption at 298K, all of the bands were disappeared.

The FTIR spectra of pyridine adsorbed on Bentonite is shown in Figure 3.15, respectively. In Figure 3.15, after evacuation at successively higher temperatures, it was observed that the band at 1445 cm^{-1} gradually became narrow and its intensity decreased. After desorption at 298, 373, 473 and 573 K, first of all, the band at 1588 cm^{-1} was interestingly shifted to 1558 cm^{-1} and the intensity of the band at 1456 cm^{-1} which was ascribed to the characteristic band as pyridine species (Lewis sites) was decreased. On the other hand, the band at 1490 cm^{-1} was gradually narrowed and its intensity decreased after desorption at 298 K. In Figure 3.15d the bands at 1634, 1558 and 1489 cm^{-1} were ascribed to the characteristic band as BPy species. On the other hand, the bands at 1622, 1456 and 1576 cm^{-1} were ascribed to the characteristic band as LPy species.
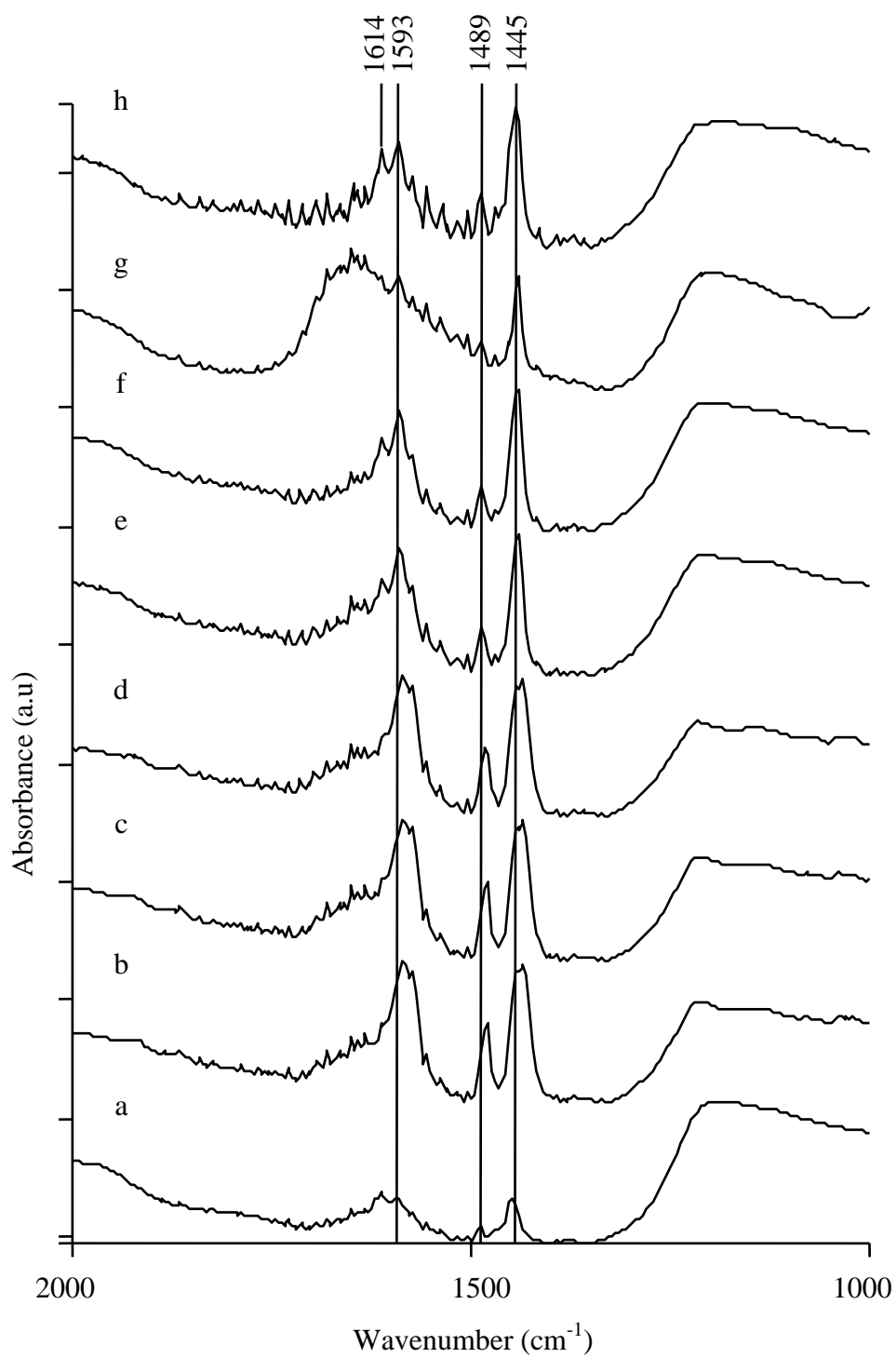
Figure 3.9 FTIR spectra of pyridine adsorbed on Siral 5 a) reference b) initial ads.
c) 15 min. ads. d) 373 K, 30 min. ads. e) 298 K, 5 min. des. f) 373 K, 10 min. des.
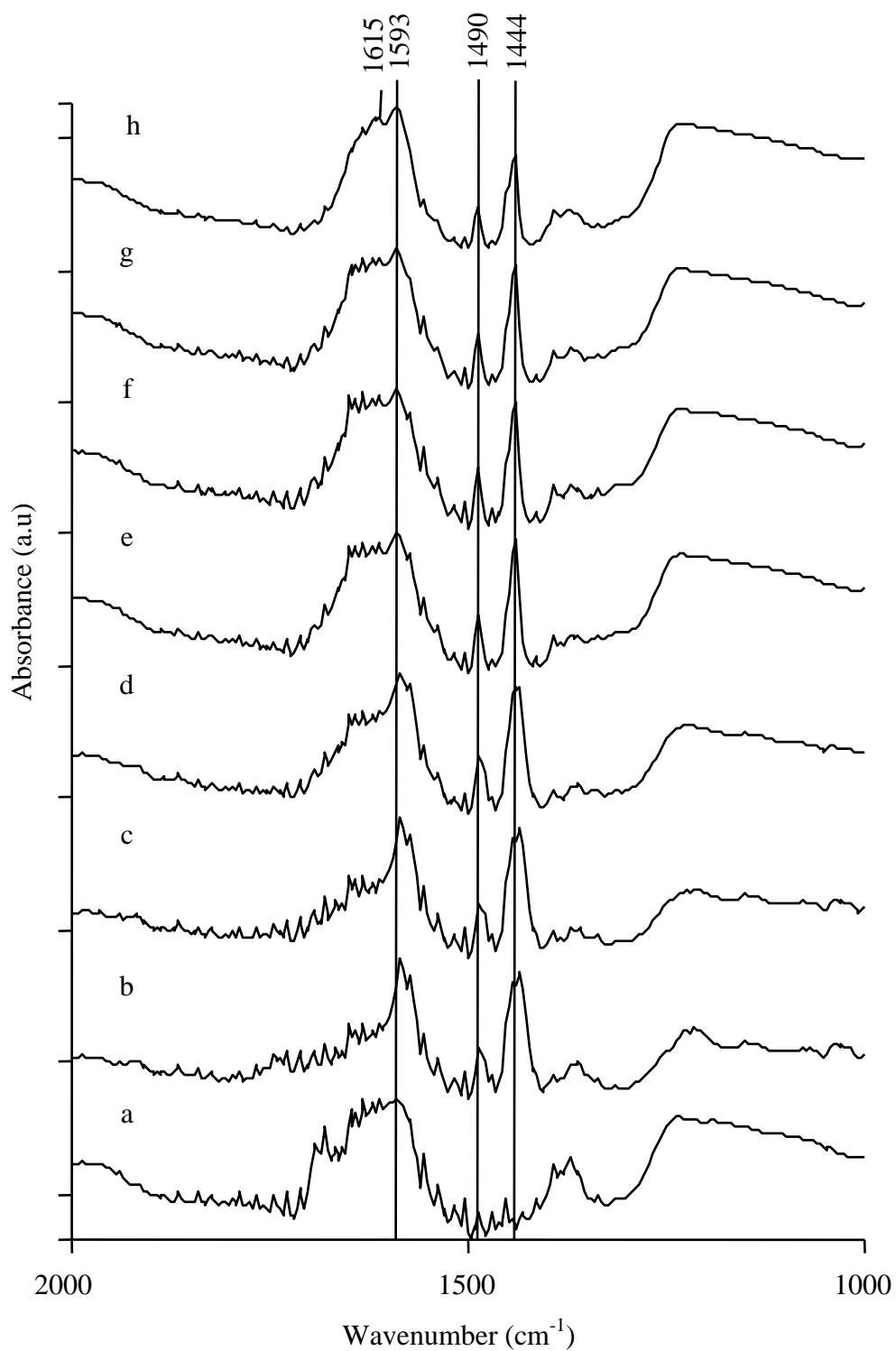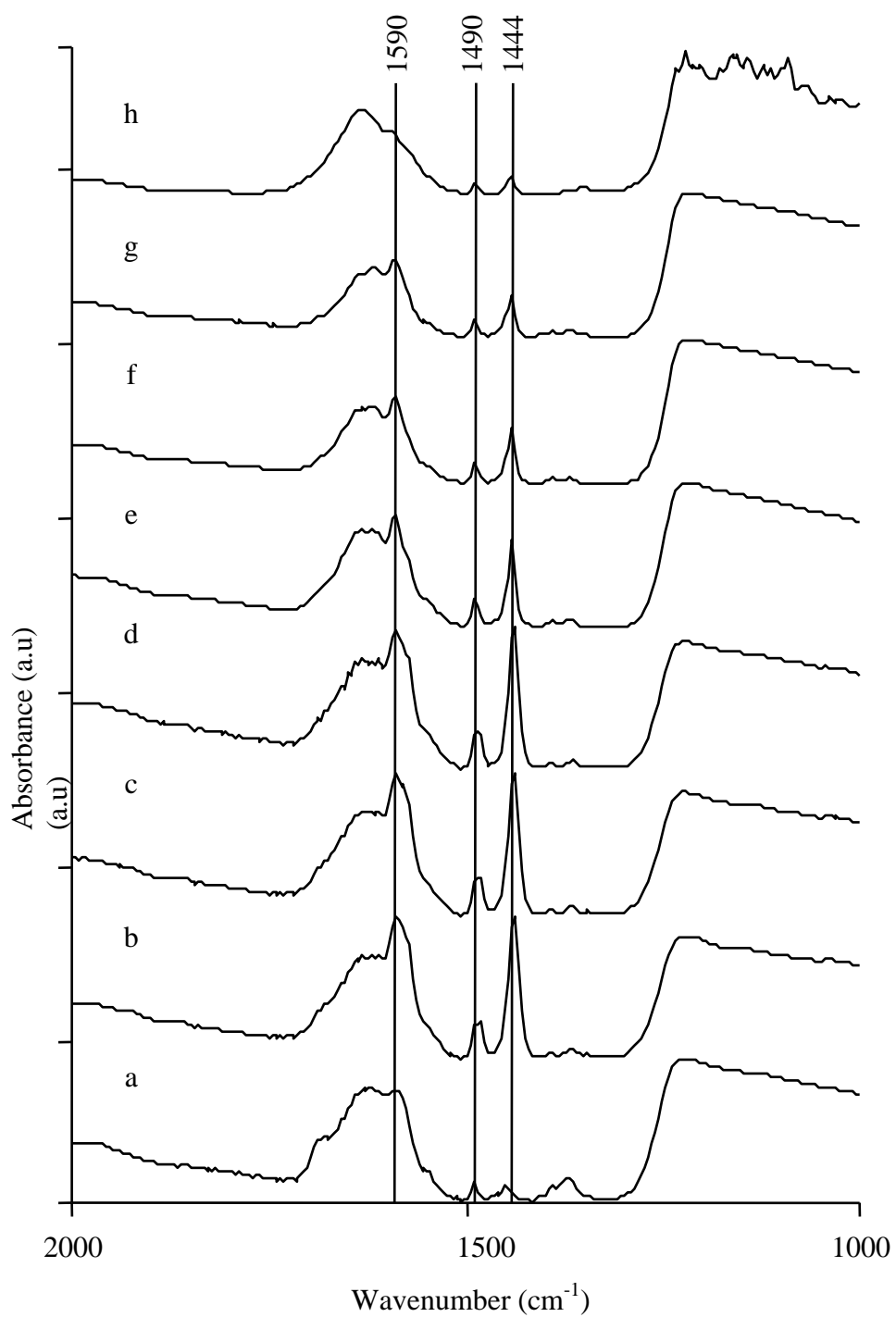g) 473 K, 10 min. des. h) 573 K, 10 min. des

Figure 3.10 FTIR spectra of pyridine adsorbed on Siral 20 a) reference b) initial ads. c) 15 min. ads. d) 373 K, 30 min. ads. e) 298 K, 5 min. des. f) 373 K, 10 min. des. g) 473 K, 10 min. des. h) 573 K, 10 min. des.

Figure 3.11 FTIR spectra of pyridine adsorbed on Siral 30 a) reference b) initial ads. c) 15 min. ads. d) 373 K, 30 min. ads. e) 298 K, 5 min. des. f) 373 K, 10 min. des. g) 473 K, 10 min. des. h) 573 K, 10 min. des.
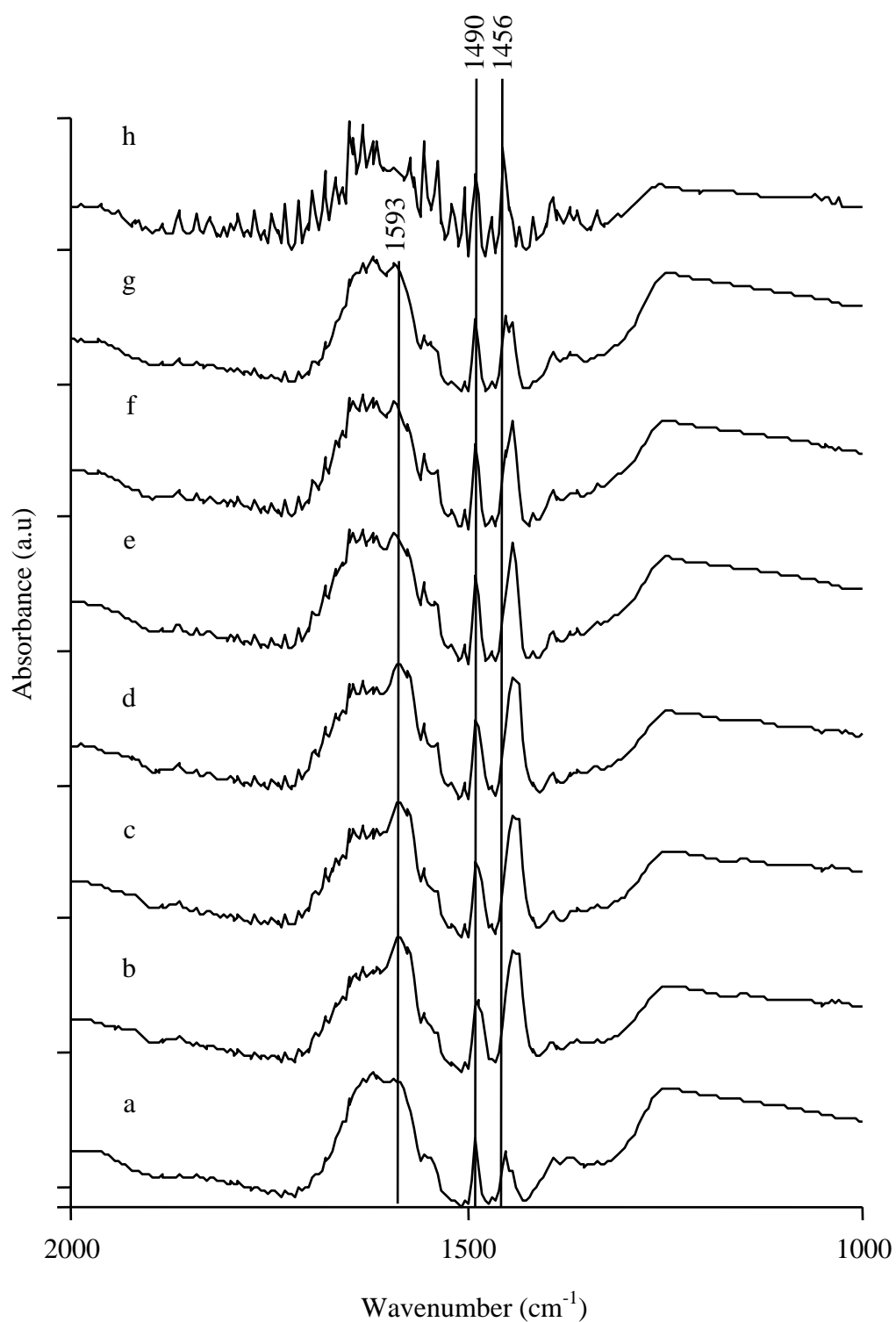
Figure 3.12 FTIR spectra of pyridine adsorbed on Siral 40 a) reference b) initial ads. c) 15 min. ads. d) 373 K, 30 min. ads. e) 298 K, 5 min. des. f) 373 K, 10 min. des. g) 473 K, 10 min. des. h) 573 K, 10 min. des
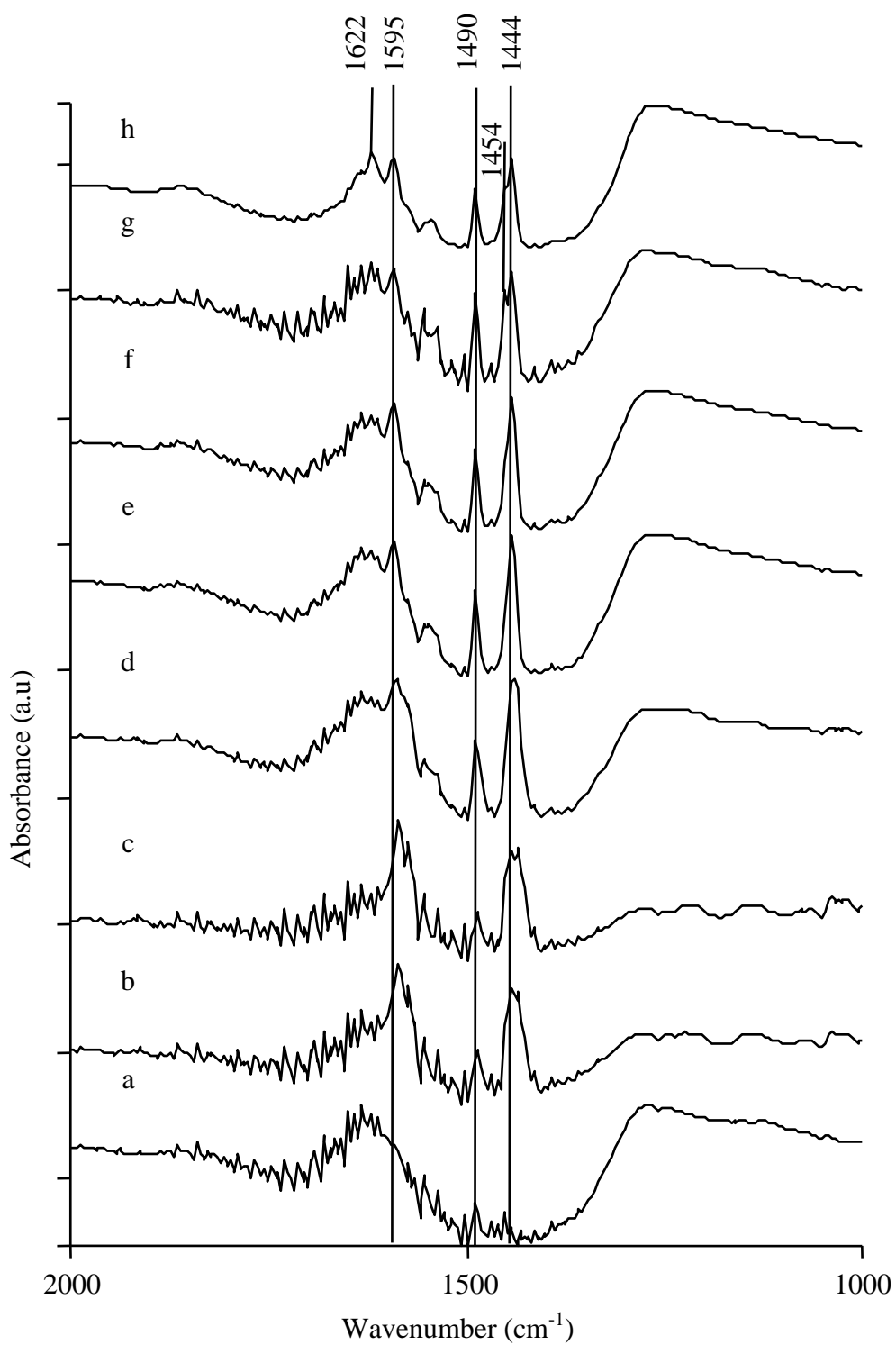
Figure 3.13 FTIR spectra of pyridine adsorbed on Siral 80 a) reference b) initial ads. c) 15 min. ads. d) 373 K, 30 min. ads. e) 298 K, 5 min. des. f) 373 K, 10 min. des. g) 473 K, 10 min. des. h) 573 K, 10 min. des.

Figure 3.14 FTIR spectra of pyridine adsorbed on Sepiolite a) reference b) initial ads. c) 15 min. ads. d) 373 K, 30 min. ads. e) 298 K, 5 min. des. f) 373 K, 10 min. des. g) 473 K, 10 min. des. h) 573 K, 10 min. des
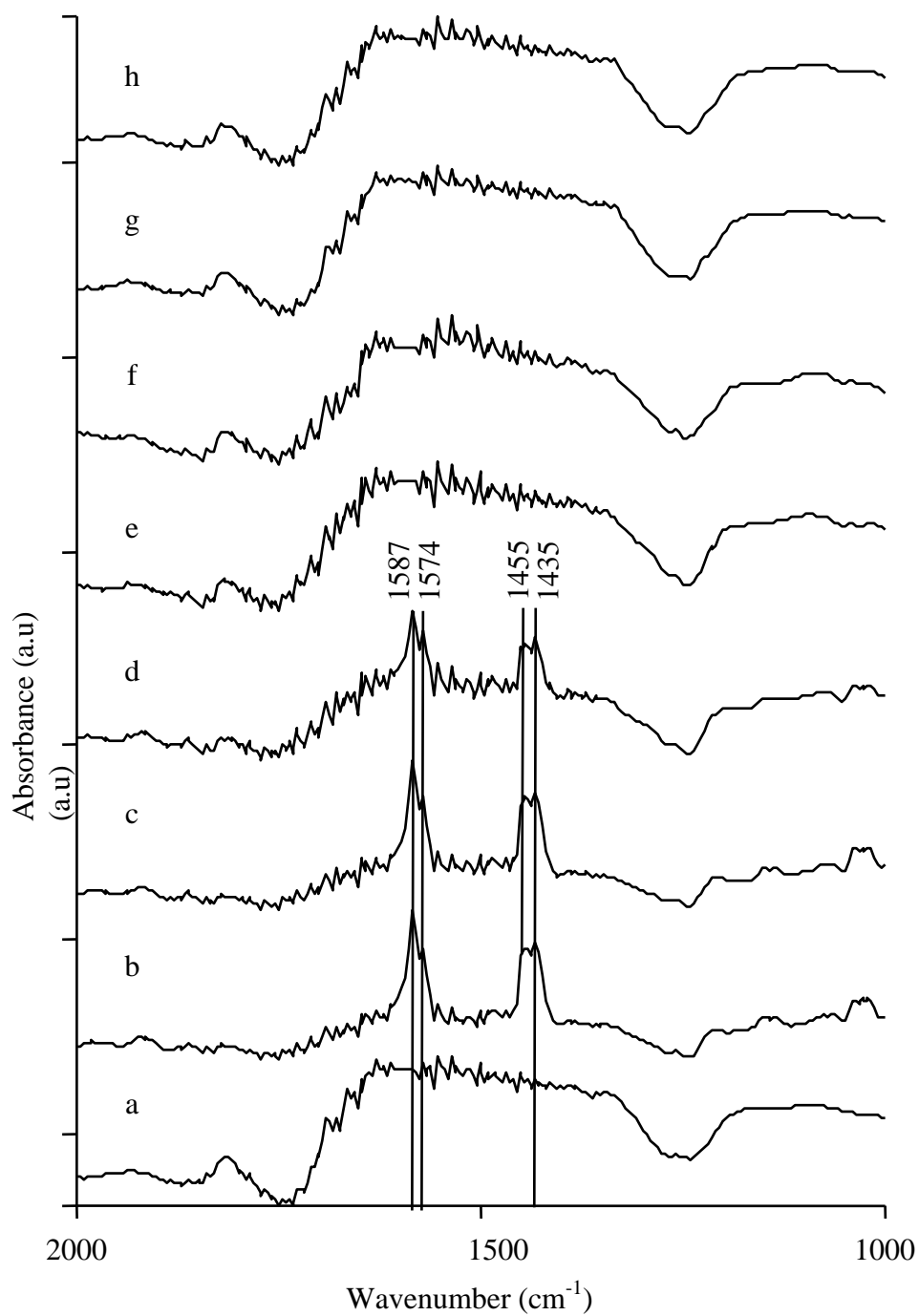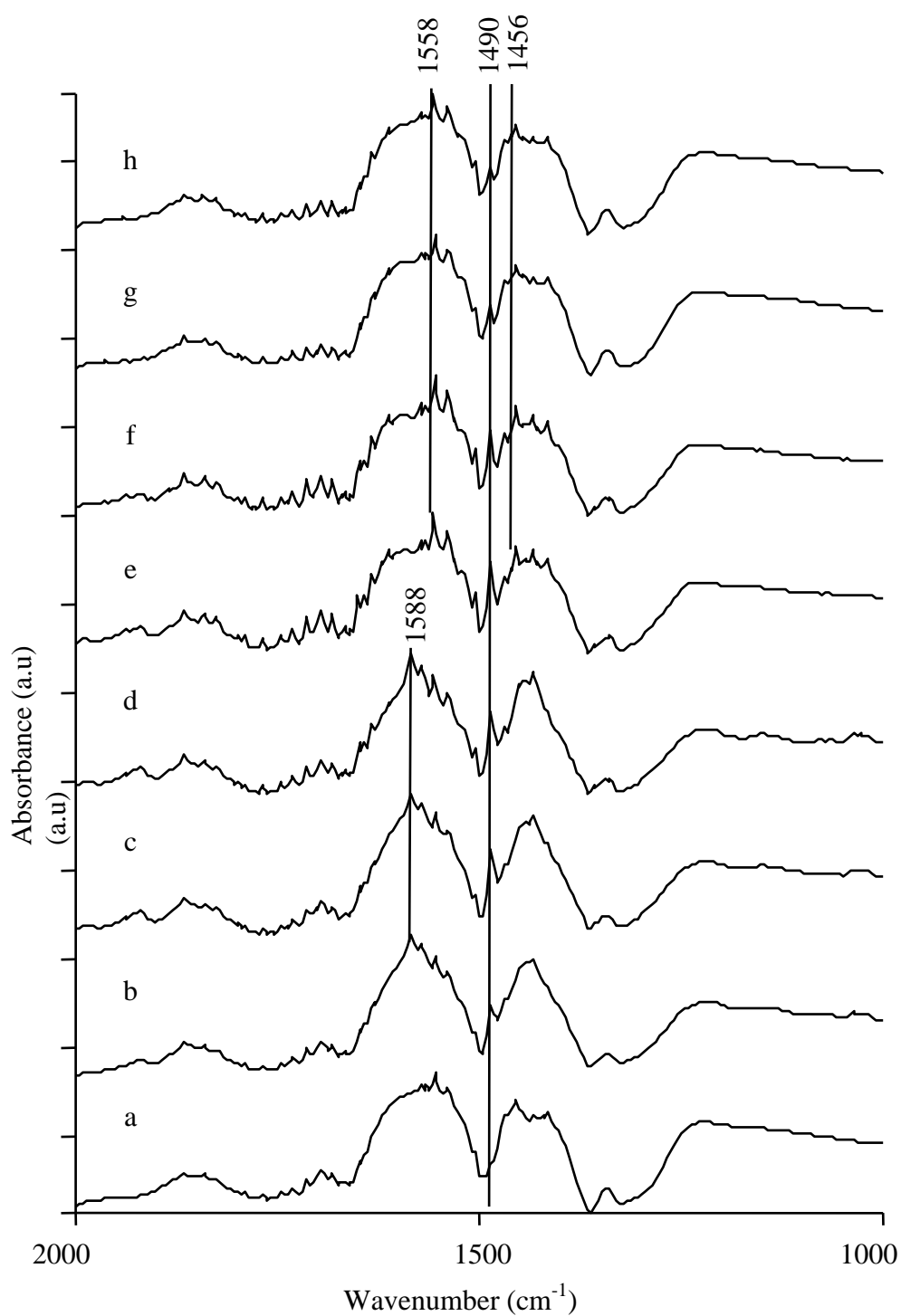
Figure 3.15 FTIR spectra of pyridine adsorbed on Bentonite a) reference b) initial ads. c) 15 min. ads. d) 373 K, 30 min. ads. e) 298 K, 5 min. des. f) 373 K, 10 min. des. g) 473 K, 10 min. des. h) 573 K, 10 min. des.

CHAPTER FOUR

CONCLUSIONS

As can be seen from the Table 3.2 that Siral 5, Siral 20, Siral 30, Siral 40, Siral 80, Sepiolite and Bentonite catalysts have an acid strength of $H_O \leq +4.8$. On the other hand, According to the results of n-butyl amine titration, the calculated total amounts of acids in the samples with the increase in SiO_2 content up to Siral 40 and then decreased sharply in the case of Siral 80 with approximately 80% of SiO_2. In liquid phase, for the clay samples, Bentonite is more acidic than Sepiolite due to the high SiO_2 content which can be seen from the Table 2.2 and Table 2.3. On the other hand, under vacuum conditions in gas phase because of high H_2O content, Sepiolite is more acidic than Bentonite under these conditions.

In the evaluation of the surface functional groups, Boehm titration results have been showed that any acidic and basic group have not been found on the surface of samples. The points of zero charge for Siral 5, Siral 20, Siral 30, Siral 40, Siral 80, Sepiolite and Bentonite catalysts range from 4.2 to 7.

FTIR spectroscopy was used successfully with pyridine as a basic probe, to determine the Brønsted and Lewis acid sites on the surface of various $SiO_2\text{-}Al_2O_3$, Sepiolite and Bentonite catalysts. In general, all samples have both Lewis and Brønsted acidity. FTIR analysis also showed that pyridine adsorption on acid solids occurs under kinetic control and that equilibrium attainment implies a redistribution of pyridine molecules between Brønsted and Lewis surface sites.

In Figures 3.9-3.15, It has been observed that the bands at 1634, 1576 and 1394 cm^{-1} which were ascribed to as pyridinium ion (Brønsted species). On the other hand, the bands at 1621, 1576, 1490 and 1456 cm^{-1} which were ascribed to as pyridine(Lewis species). In the evaluation of the pyridine adsorption-desorption spectra of the samples, it was aimed to compare the data by thinking the chemical contents of the samples. This means that the content of $SiO_2\text{-}Al_2O_3$. For this reason,

it has been chosen Siral 40, Sepiolite and Bentonite due to approximately the same SiO$_2$ percentage.

The FTIR spectra of pyridine adsorbed on Siral 40 is shown in Figure 3.12. In Figure 3.12, after evacuation (desorption of the adsorbed pyridine onto sample) at successively higher temperatures, it was observed that the band at 1444 cm^{-1} was gradually narrowed, its intensity decreased, and the band shifted to 1456 cm^{-1}. After desorption at 573 K it was observed that the band at 1490 cm^{-1} which was ascribed to the characteristic band as pyridinium ion and pyridine (Lewis species). Appearance of this band still after desorption at 573 K reflects the strong interaction of pyridine onto surface acid sites (Brønsted and also Lewis sites). This may be attributed to the chemical adsorption of pyridine onto surface of the samples.

On the other hand, the FTIR spectra of pyridine adsorbed on Sepiolite is shown in Figure 3.14. It has been seen from this figure that after evacuation at successively higher temperatures, it was only observed that the band at 1557 cm^{-1} was gradually narrowed, its intensity decreased. As can be seen also in Figure 3.14e, after desorption at 298K, all of the bands were disappeared. This may be due the weak interaction between pyridine and surface acid sites. It can be also said that the possible interaction is due to physical adsorption.

Afterwards, the FTIR spectra of pyridine adsorbed on Bentonite is shown in Figure 3.15. In Figure 3.15, after evacuation at successively higher temperatures, it was observed that the band at 1445 cm^{-1} gradually became narrow and its intensity decreased. After desorption at 298, 373, 473 and 573 K, first of all, the band at 1588 cm^{-1} was interestingly shifted to 1558 cm^{-1} and the intensity of the band at 1456 cm^{-1} which is ascribed to as Pyridine species (Lewis sites) was decreased. On the other hand, the band at 1490 cm^{-1} was gradually narrowed and its intensity decreased after desorption at 298 K. This might be indicated the sorption mechanism was valid as far as the surface structures. As a result, it can be said that the Lewis sites predominate in all the silica-aluminas, but that a wide range in the ratio of Lewis to Brønsted sites still exists.

REFERENCES

Aluminium Silicate. (n.d). Retrieved April 15, 2011, from
    http://www.tutorvista.com/chemistry/aluminium-silicate

Barzetti., T., Selli, E., Moscotti, D., & Forni, L. (1996). Pyridine and ammonia as
    probes for FTIR analysis of solid acid catalysts. *Journal of Chemical Society,
    Faraday Transactions*, *92(8)*, 1401-1407.

Basila, M. R., Kantner, T. R., & Rhee, K. H. (1964). The nature of the acidic sites on
    a silica-alumina. Characterization by infrared spectroscopic studies of
    trimethylamine and pyridine chemisorption. *Journal of Physical Chemistry*,
    68(11), 3197-3207.

Benesi, H. A. (1957). Acidity of catalyst surfaces. II. Amine titration using Hammett
    indicators. *Journal of Physical Chemistry, 61*, 970-973.

Bentonite. (n. d.). Retrieved April 15, 2011, from
    http://www.imaeu.org/fileadmin/downloads/publications/factsheets/Bentonite_An-
    WEB-2011.pdf

Bjerrum, J., & Sansoni, B. (1951). Die entwicklungsgeschichte des säure-
    basenbegriffes und über die zweckmäßigkeit der einführung eines besonderen
    antibasenbegriffes neben dem säurebegriff. *Naturwissenschaften*, *38*, 461-464.

Boehm, H.P. (1994). Some aspects of the surface chemistry of carbon blacks and
    other carbons. *Carbon*, *32*, 759-769.

Bouberka, Z., Kacha, S., Kameche, M., Elmaleh, S., & Derriche, Z. (2005). Sorption
    study of an acid dye from an aqueous solutions using modified clays. *Journal of
    Hazardous Materials B*, *119*, 117-124.

Bourne, K. H., Cannings, F.R., & Pitkethly, R.C. (1970). Acid sites in a mixed-oxide system. The structure and properties of acid sites in a Mixed-Oxide system I. Synthesis and infrared characterization. *Journal of Physical Chemistry*, *74*, 2197-2205.

Brønsted, J. N. (1926). The acid-basic function of molecules and its dependency on the electric charge type. *The Journal of Physical Chemistry*, *30*, 777-790.

Cannings, F.R. (1968). Acidic sites on mordenite: an infrared study of adsorbed pyridine. *Journal of Physical Chemistry*, *72*, 4691-4693.

Catalytic Processes and Materials. (n. d.). Retrieved May 15, 2011, from http://www.utwente.nl/tnw/cpm/

Cook, D. (1961). Vibrational spectra of pyridinium salts. *Canadian Journal of Chemistry*, *39*, 2009-2024.

Darder M., Blanco, M., Aranda, P., Aznar, J. A., Bravo, J., & Hitzky, E. R. (2006). Microfibrous chitosan sepiolite nanocomposites. *Chemistry of Materials*, *18*, 1602-1610.

Datka, J., Gil, B., & Kubacka, A. (1995). Acid properties of NaH-mordenites: Infrared spectroscopic studies of ammonia sorption. *Zeolites*, *15*, 501-506.

Datka, J., Turek, A. M., Jehng, J. H., & Wachs, I. E. (1992). Acidic properties of supported niobium oxide catalysts: An infrared spectroscopy investigation. *Journal of Catalysis*, *135*, 186-199.

Emeis C. A. (1993). Determination of integrated molar extinction coefficients for infrared absorption bands of pyridine adsorbed on solid acid catalysts. *Journal of Catalysis*, *141*, 347-354.

Flood, H., & Förland, T. (1947). The acidic and basic properties of oxides. *Acta Chemica Scandinavica*, *1*, 592-604

Flood, H., & Förland, T. (1947). The acidic and basic properties of Oxides. II. The thermal decomposition of pyrosulphates. *Acta Chemica Scandinavica*, *1*, 781-789.

Franklin, E. C. (1905). Reactions in liquid ammonia. *Journal of the American Chemical Society*, *27*, 820-851.

Germann, A. F. O. (1925). A general theory of solvent systems. *Journal of the American Chemical Society*, *47*, 2461-2468.

Gill, N. S., Nuttall, R. H., Scaife, D. E. & Sharp, D. W. A. (1961). Infrared spectra of pyridine complexes and pyridinium salts. *Journal of Inorganic and Nuclear Chemistry*, 18, 79-87.

Hughes, T. R., & White, H. M. (1967). A study of the surface structure of decationized Y zeolite by quantitative infrared spectroscopy. *Journal of Physical Chemistry*, *71(7)*, 2192-2201.

Jacobs, P. A., & Uytterhoeven, J. B. (1972). Quantitative infrared spectroscopy of amines in synthetic zeolites X and Y : I. Alkylammonium Y zeolites as precursors of acid hydroxyls in deaminated zeolites Y. *Journal of Catalysis*, *26*, 175-190.

Johnson, R. E., Norris, T. H., & Huston, J. L. (1951). Acid-base exchange reactions in liquid sulfur dioxide. *Journal of the American Chemical Society*, *73*, 3052-3055.

Keith, K. S. (2000). *Characterization and permeability of sepiolite, palygorskite and other commercial clays and their applicability for use as impermeable barriers in waste disposal*. Ph.D. Thesis Bloomington, Indiana University.

Khabtou, S., Chevreau T., & Lavalley, J. C. (1994). Quantitative infrared study of the distinct acidic hydroxyl groups contained in modified Y zeolites. *Microporous Materials*, 3, 133-148.

Kijenski, J., & Baiker, A. (1989). Acidic sites on catalyst surfaces and their determination. *Catalysis Today. 5*, 1-120.

Kiselev, A. V., & Uvarov, A. V. (1967). Infrared spectra and electron spin resonance of aluminium, silicon and titanium oxides and of adsorbed substances. *Surface Science*, *6*, 399-421.

Kiviat, F. E., & Petrakis, L. (1973). Surface acidity of transition metal modified aluminas.Infrared and nuclear magnetic resonance investigation of adsorbed pyridine. *Journal of Physical Chemistry*, *77*, 1232-1239.

Knözinger, H. (1976). Specific poisoning and characterization of catalytically active oxide surfaces. *Advances in Catalysis*, *25*, 184-271.

Kubilay, S., Gürkan, R., Savran, A., & Sahan, T. (2007). Performance of activated carbon and bentonite for adsorption of amoxicillin from wastewater: Mechanisms, isotherms and kinetics. *Adsorption*, *13*, 41–51.

Lewis, G. N. (1938). Acids and Bases. *Journal of the Franklin Institute*, *226*, 293.

Lindemann, R., & Zundel, G. (1977). Polarizability, proton transfer and symmetry of energy surfaces of carboxylic acid—*N*-base hydrogen bonds. Infrared investigations. *Journal of Chemical Society, Faraday Transactions II, 73*, 788-803.

Makarova, M. A., Karim, K., & Dwyer, J. (1995). Limitation in the application of pyridine for quantitative studies of Brønsted acidity in relatively aluminous zeolites. *Microporous Materials*, *4*, 243-246.

Mapes, J. E., & Eischens, R . P. (1954). The Infrared Spectra of Ammonia Chemisorbed on Cracking Catalysts. *Journal of Physical Chemistry*, *58*, 1059-1062.

Montmorillonite. (n. d.). Retrieved May 12, 2011, from (http://pubs.usgs.gov/of/2001/of01-041/htmldocs/images/monstru.jpg)

Parry, E. P. (1963). An infrared study of pyridine adsorbed on acidic solids. Characterization of surface acidity. *Journal of Catalysis*, *2*, 371-379.

Pearson, R. G. (1963). Hard and soft acids and bases. *Journal of American Chemical Society*, *85*, 3533-3539.

Putra, E. K., Pranowo R., Sunarso J., Indraswati N., & Ismadji S. (2009). Performance of activated carbon and bentonite for adsorption of amoxicillin from wastewater: Mechanisms, isotherms and kinetics. *Water Research*, *43*, 2419–2430.

Rajagopal, S., Marzari, J. A., & Miranda, R. (1995). Silica- Alumina-Supported Mo oxide catalysts: Genesis and demise of Brønsted-Lewis acidity. *Journal of Catalysis, 151*, 192-203.

Richardson, R.L., & Benson, S.W. (1957). A study of the surface acidity of cracking catalyst. *The Journal of Physical Chemistry*, *61*, 405-411.

Saavedra, R. F., Aranda, P., & Hitzky, E. R. (2004). Templated synthesis of carbon nanofibers from polyacrilonitrile using sepiolite. *Advanced Functional Materials*, *14*, 72-82.

Selli, E., & Forni, L. (1999). Comparison between the surface acidity of solid catalysts determined by TPD and FTIR analysis of pre-adsorbed pyridine. *Microporous and Mesoporous Materials*, *31*, 129-140.

Sepiolite and palygorskite. (2 October 2001). Retrieved August 25, 2010, from *U. S. Geological Survey Open-File Report 01-041, A Laboratory Manual for X-Ray Powder Diffraction*, http://pubs.usgs.gov/of/2001/of01-041/htmldocs/clays/seppaly.htm

Sepiolite. (n.d.). Retrieved April 14, 2011, from http://www.imaeu.org/fileadmin/downloads/publications/factsheets/Sepiolitemine ralfact sheet EN.pdf

Tanabe K. (1970). *Solid Acids and Bases, their catalytic properties*. New York: Academic Press

Tanabe K., Hattori, H. (1976). The synthesis of solid super acids and the activity for the reactions of butane and isobutane. *Chemistry Letters, (6)*, 625-626.

Tanabe, K. (1981). *Catalysis In Science and Technology Vol. 2, Chapt. 5.* Berlin: Springer-Verlag.

Tanabe, K. (1985). *Catalysis by Acids and Bases.* Amsterdam: Elsevier

Tanabe, K., Misono, M., Ono, Y., Hattori, H. (1989). *Studies in Surface Science and Catalysis Vol. 51, New Solid Acids and Bases Their Catalytic Properties*. Amsterdam: Elsevier

Thomas, C. L. (1949). Chemistry of cracking catalysts. *Industrial & Engineering Chemistry*, *41 (11)*, 2564–2573.

Toles, C. A., Marshall W. E., & Johns, M. M. (1999). Surface functional groups on acid-activated nut shell carbons. *Carbon*, *37*, 1207–1214.

Turek, A. M., Wachs, I. E., & DeCanio, E. (1992). Acidic properties of alumina-supported metal oxide catalysts: an infrared spectroscopy study. *Journal of Physical Chemistry*, *96*, 5000-5007.

Walling, C. (1950). The acid strength of surfaces. *Journal of American Chemical Society*, *72*, 1164-1168.

Yashima, T., & Hara, N. (1972). Infrared study of cation-exchanged mordenites and Y faujasites adsorbed with ammonia and pyridine. *Journal of Catalysis*, *27*, 329-333.

Yurdakoç, M., Akçay, M.,Tonbul, Y. & Yurdakoç, K. (1999). Acidity of silica-alumina catalysts by amine titration using Hammett indicators and FT-IR study of pyridine adsorption. *Turkish Journal of Chemistry*, *23*, 319-327.

Zerbi, G., Crawford, B., & Overend, J. (1963). Normal coordinates of the planar vibrations of pyridine and its deuteroisomers with a modified Urey—Bradley Force Field. *Journal of Chemical Physics*, *38*, 127-134.